



Energy, Mines and
Resources Canada

Énergie, Mines et
Ressources Canada

Earth Physics Branch

Direction de la physique du globe

1 Observatory Crescent
Ottawa Canada
K1A 0Y3

1 Place de l'Observatoire
Ottawa Canada
K1A 0Y3

**Geothermal Service
of Canada**

**Service géothermique
du Canada**

TEM SURVEY TO MAP THE DISTRIBUTION OF PERMAFROST,
SEISMIC LINE 86026, TUKTOYAKTUK, N.W.T.

Geo-Physi-Con Co. Ltd.

Earth Physics Branch Open File Number 86-9
Dossier public de la Direction de la Physique du Globe No. 86-9

NOTE FOR REPRODUCTION

REPRODUCTION INTERDITE

Department of Energy, Mines &
Resources Canada
Earth Physics Branch
Division of Gravity, Geothermics
and Geodynamics

Ministère de L'Énergie, des Mines
et des Ressources du Canada
Direction de la physique de globe
Division de la gravité, géothermie
et géodynamique

pp: 70
Price/Prix: \$21.94

This document was produced
by scanning the original publication.

Ce document est le produit d'une
numérisation par balayage
de la publication originale.

ABSTRACT

In a jointly supported project for Energy, Mines and Resources and Home Oil, Geo-Physi-Con conducted a transient electromagnetic sounding survey along a 11 km line south of Tuktoyaktuk, N.W.T. The project was conducted to test the use of electromagnetic methods in developing static corrections for seismic surveys. Electromagnetic results reported here propose a two-layer model for permafrost 300 to 500 m thick. The model shows good agreement with down-hole electrical logs.

RESUME

La compagnie Geo-Physi-Con a réalisé des sondages électromagnétiques transitoires le long d'une traverse d'onze kilomètres située au sud de Tuktoyaktuk, T.N.-O. Ce projet, soutenu conjointement par Énergie, Mines et Ressources et Home Oil, a été entrepris pour évaluer l'utilité des méthodes électromagnétiques envers le développement de corrections statiques pour la prospection sismique. Les résultats de cette étude électromagnétique suggèrent un modèle à deux couches du pergélisol de 300 à 500 m en épaisseur. Ce modèle est en bon accord avec les diagraphies électriques.

GEO-PHYSI-CON

TEM SURVEY TO MAP
THE DISTRIBUTION OF PERMAFROST
SEISMIC LINE 86026
TUKTOYAKTUK, N.W.T.

Prepared For

DEPT. OF ENERGY, MINES & RESOURCES
EARTH PHYSICS BRANCH
OTTAWA, ONTARIO
and
HOME OIL COMPANY LIMITED
CALGARY, ALBERTA

Prepared By

GEO-PHYSI-CON CO. LTD.
CALGARY, ALBERTA

JUNE 1985
C84-10

TABLE OF CONTENTS

	<u>Page</u>
1.0 INTRODUCTION	1
2.0 LOGISTICS	2
3.0 DATA ACQUISITION	3
4.0 INSTRUMENTATION AND THEORY	3
4.1 EM37 - Transient System	3
4.1.1 Definition of Apparent Resistivity	8
4.1.2 Correction Factors for Ramp Time	13
4.1.3 Influence of Turn-On Time and Ramp Time of Previous Pulse.	15
4.2 EM31 and EM34-3 - Fixed Frequency Systems	16
5.0 BASIC PRINCIPLES OF USE OF INFORMATION ON PERMAFROST DISTRIBUTION FROM TEM DATA FOR CDP STATIC CORRECTION	19
6.0 RESULTS	20
6.1 Geoelectric Structure	20
6.2 EM Data	21
6.3 Distortion of Apparent Resistivity Curves	21
6.4 Interpreted Section	22
7.0 CONCLUSIONS	23
8.0 RECOMMENDATIONS	25
REFERENCES	27

1.0 INTRODUCTION

During March 1985 a geophysical survey was performed at a site on land immediately south of Tuktoyaktuk, N.W.T. The survey was conducted using the methods of transient electromagnetic (TEM) soundings and fixed frequency electromagnetic induction (EM) at low induction number. The measurements were performed along a seismic survey line and constitute part of a test program. The objective of the program was to investigate the applicability of the information on permafrost distribution obtained from electrical methods to assist seismic data processing in accounting for the influence of frozen ground.

Figure 1 shows the location of the survey area. Figure 2 shows location of the survey line.

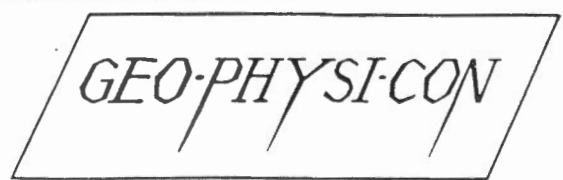
This report describes all aspects of the electrical surveys. The results of joint interpretation of seismic and electrical data will be presented at a later date after further investigations are carried out by personnel of Petro Canada Resources.



LEGEND

- Project Area
- Provincial Boundaries
- International Boundaries

SCALE

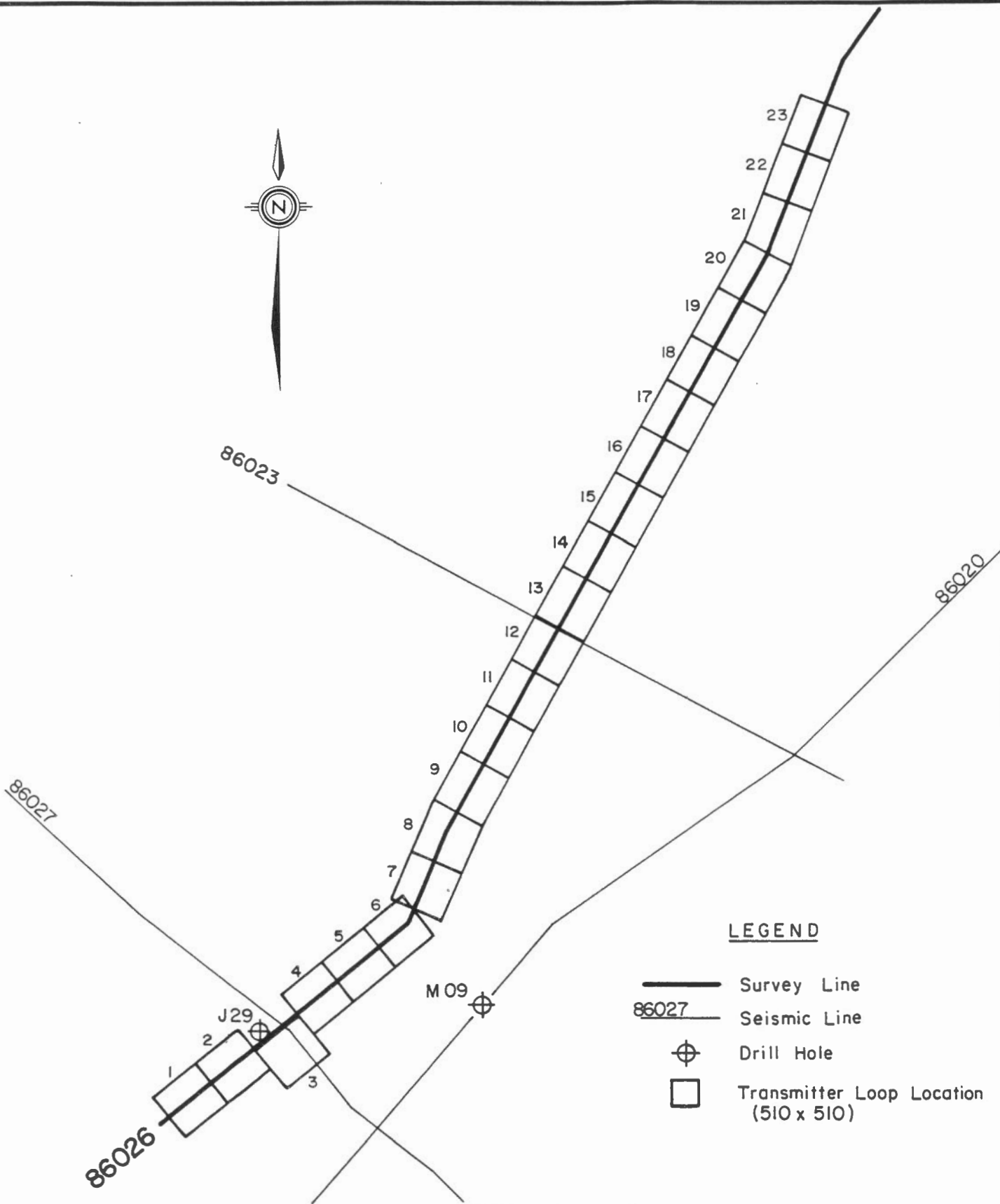


ENGINEERING GEOPHYSICAL CONSULTANTS





SURVEYED SITE LOCATION

C85-10

Figure 1



LEGEND

-  Survey Line
-  Seismic Line
-  Drill Hole
-  Transmitter Loop Location (510 x 510)

GEO-PHYSI-CON

SURVEYED LINE LOCATION

2.0 LOGISTICS

The test survey was performed by a five man crew during the period March 20 to 31, 1985. Mobilization and demobilization between Tuktoyaktuk and Calgary took place on March 19 and April 1.

The crew travelled to and from the survey site daily by locally rented vehicles.

Three Skidoos were used to lay out and take up cable and to move the generator, transmitter and receiver for the TEM work. Over the course of the survey, 23 stations (approximately 11.5 km) were surveyed with two transmitter loop sizes.

All fixed frequency EM measurements were recorded by the crew progressing by snowshoe. About 11.5 kms of EM survey at 60 m and 90 m spacings and six effective depths of exploration were recorded.

Accommodations and fuel were supplied by Esso Resources Canada Ltd. at their Tuktoyaktuk base camp.

3.0 DATA ACQUISITION

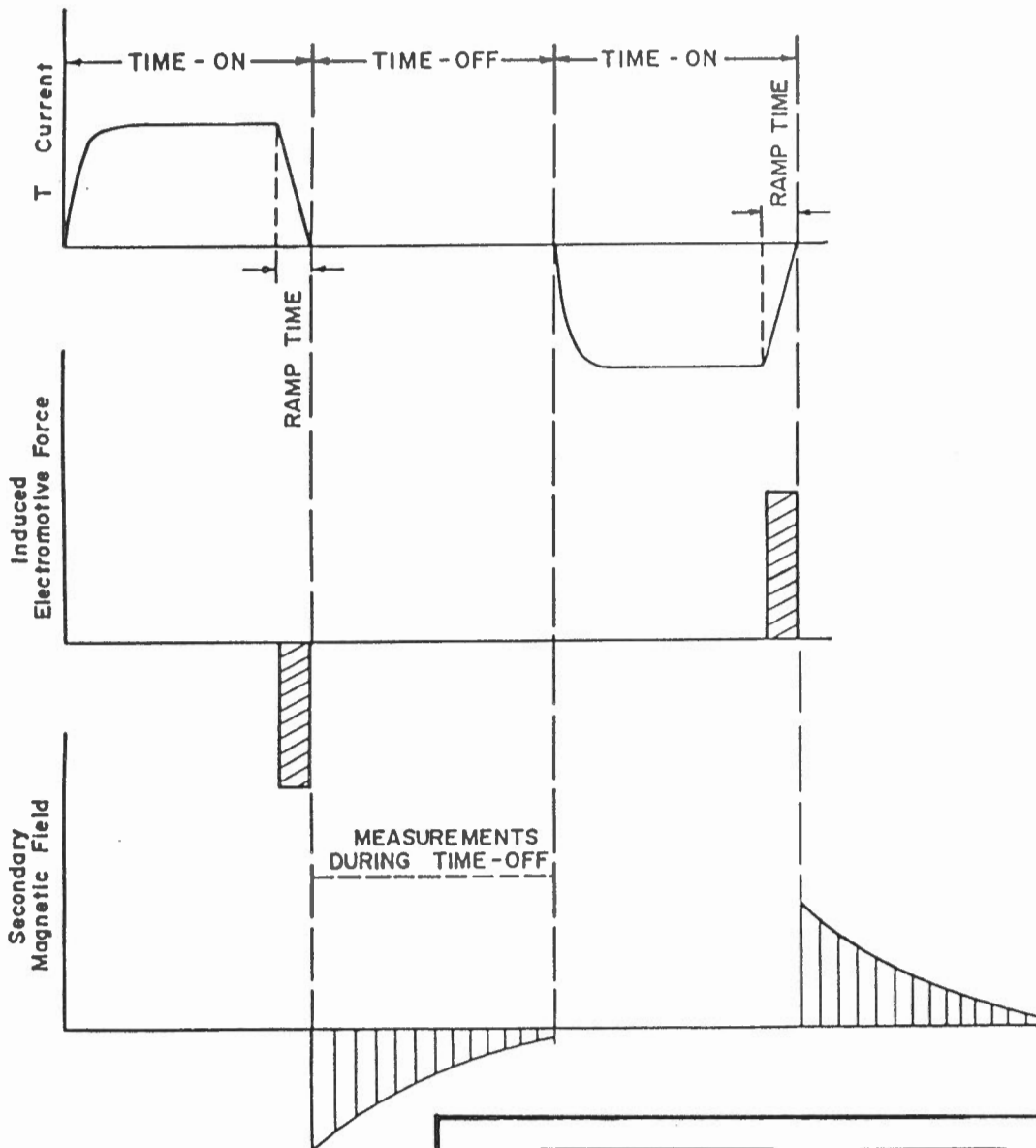
Measurements using the TEM method were recorded at stations separated by 510 m intervals. At each station soundings were performed for transmitter loop sizes of 510 m by 510 m and 200 m by 200 m. The large loop size was used to gather data identifying the base of permafrost at each station. The small loop size was used to identify lateral discontinuities and complex layering that were less well evidenced in the large loop data.

At each site EM measurements were taken along a line intersecting the TEM stations. EM data was gathered using six different measurement modes. Table 1 lists the exploration modes, station spacing and effective depth of exploration.

4.0 INSTRUMENTATION AND THEORY

4.1 EM37 - Transient System

The transient system consists of a transmitter and receiver. The transmitter configuration used was a horizontal non-grounded loop. Figure 3 shows the behavior of the current



a) CURRENT IN TRANSMITTER LOOP

b) INDUCED ELECTROMOTIVE FORCE CAUSED BY T CURRENT

c) SECONDARY MAGNETIC FIELD CAUSED BY EDDY CURRENTS

GEO-PHYSI-CON

SYSTEM WAVEFORMS

TABLE 1 - EM MEASUREMENT MODES RECORDED

MEASUREMENT MODE	STATION SPACING	EFFECTIVE EXPLORATION DEPTH
EM31VG - vertical coplanar loop mode at ground level	50 m	2.0
EM31HZ - horizontal coplanar loop mode at hip level	50 m	4.0
EM31HG - horizontal coplanar loop mode at ground level	50 m	5.0
EM34-20V - vertical coplanar loop mode, 20 m loop separation	100 m	11.5
EM34-40V - vertical coplanar loop mode, 40 m loop separation	100 m	23.0
EM34-40H - horizontal coplanar loop mode, 40 m loop separation	100 m	50.0

GEO-PHYSI-CON

wave form in the transmitter loop as a function of time. The system has equal periods of time-on and time-off. Three base frequencies for pulse repetition, 30 Hz (HF), 3 Hz (LF) and 0.3 Hz (VLF) can be employed. This gives time-on and time-off periods of 8.33 ms, 83.3 ms and 833 ms, respectively. The turn-on pulse is approximately of the form:

$$J(t) = J_0(1 - \exp(-t/\tau_0))$$

where $J(t)$ is the current at time t after turn-on,
 J_0 is the peak current, and
 τ_0 is an on-time constant

The time constant τ_0 depends mainly on the size of the transmitter loop used and is approximately 0.5 millisecond for a 510 m by 510 m loop.

The turn-off ramp is linear. The ramp time is experimentally measured on the instrument. The ramp time is a function of transmitter loop size and peak current. It varies from approximately 150 microseconds for a 200 m x 200 m loop to 500 microseconds for a 510 m x 510 m loop.

GEO-PHYSI-CON

The receiving element is a multi-turn coil that measures the electromotive force caused by the time derivative of the secondary magnetic field. The receiver can occupy stations inside as well as outside the loop. For the present survey, measurements were made only with the receiver in the centre of the transmitter loop and at base frequencies of 30 Hz and 3 Hz.

Table 2 lists the positions and widths of the time gates of the receiver at high, low and very low frequency. The time is in reference to the bottom of the turn-off ramp (see illustration Table 2). To precisely reference the gate locations to the end of the ramp, the ramp time measured on the transmitter is set on the receiver.

Synchronization of the transmitter and receiver is achieved using high stability (oven controlled) quartz crystals. This method of synchronization required phasing of the crystals each time the transmitter frequency is changed or the transmitter is shut down. During transmitter shut down the oven temperatures are maintained for both the transmitter and receiver using the receiver battery pack.

TABLE 2 - LIST OF TIME OF GATE CENTRES AND GATE WIDTHS

CHANNEL NO.	GATE CENTRE			GATE WIDTH		
	HF	LF	VLF	HF	LF	VLF
1	0.089 ms	0.89 ms	8.9 ms	0.018 ms	0.18 ms	1.8 ms
2	0.100	1.00	10.0	0.024	0.24	2.4
3	0.140	1.40	14.0	0.037	0.37	3.7
4	0.177	1.77	17.7	0.036	0.36	3.6
5	0.220	2.20	22.0	0.050	0.50	5.0
6	0.280	2.80	28.0	0.072	0.72	7.2
7	0.355	3.55	35.5	0.076	0.76	7.6
8	0.443	4.43	44.3	0.100	1.00	10.0
9	0.564	5.64	56.4	0.142	1.42	14.2
10	0.713	7.13	71.3	0.156	1.56	15.6
11	0.881	8.81	88.1	0.180	1.80	18.0
12	1.096	10.96	109.6	0.250	2.50	25.0
13	1.411	14.11	141.1	0.380	3.80	38.0
14	1.795	17.95	179.5	0.390	3.90	39.0
15	2.224	22.24	222.4	0.500	5.00	50.0
16	2.850	28.50	285.0	0.720	7.20	72.0
17	3.600	36.00	360.0	0.780	7.80	78.0
18	4.490	44.90	449.0	1.080	10.80	108.0
19	5.700	57.00	570.0	1.420	14.20	142.0
20	7.190	71.90	719.0	1.560	15.60	156.0

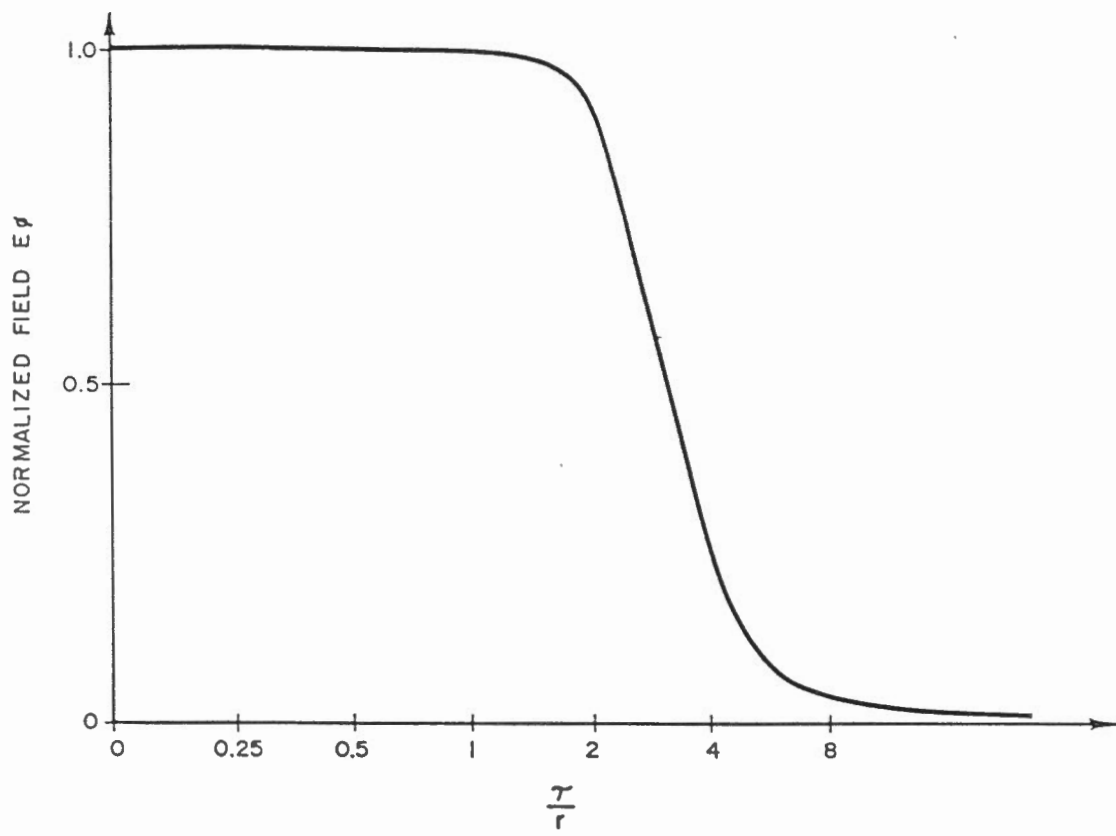
Detailed manufacturer's specifications on the instrument are given in Appendix A.

4.1.1 Definition of Apparent Resistivity

It is common in electrical and electromagnetic prospecting (especially in soundings) not to work with the behavior of field, but to convert the measured field components into apparent resistivities. This approach has also been used for many years in transient electromagnetic soundings.

It has been shown that the system, consisting of a square transmitter loop with the receiver at its centre, is completely equivalent in the time range employed to a system consisting of a magnetic dipole transmitter and electric dipole receiver. As a result, the theory developed for the latter case above is valid for the system used, provided that the distance between the dipoles is equal to $L/\sqrt{\pi}$. L , where L is the length of a side of the transmitter loop.

To understand the definitions of apparent resistivity used in this report consider the behavior of the field induced in a homogeneous half-space. In Figure 4 the tangential electrical field component is plotted versus the parameter, T/r ,



GEO-PHYSI-CON

ENGINEERING GEOPHYSICAL CONSULTANTS

BEHAVIOR OF $E\phi$

C 85-10

Figure 4

$$\tau = \sqrt{2\pi\rho t 10^7} \quad [1]$$

where r is distance between dipole and point of measurement in metres,

ρ is the resistivity of half-space in ohm-m, and

t is time after turn-off in seconds

The general behavior of the field is a complex function, but it has been shown that at values of $\tau/r < 2$, and at $\tau/r > 10$, simple asymptotic expressions describe the field to good accuracy (5%). At early stage ($\tau/r < 2$) the field is independent of time and the asymptotic expression is given by:

$$E_{\theta} = \frac{3 m \rho}{2 \pi r^4} \quad [2]$$

where m is the moment of the transmitting dipole in amperes-m².

At late stage ($\tau/r > 10$) the field is given by the expression:

$$E_{\phi} = \frac{mr\mu^{5/2}}{40\pi^{3/2} \rho^{3/2} t^{5/2}} \quad [3]$$

where μ is magnetic susceptibility of free space in henry/m.

Clearly, two different definitions of apparent resistivity can be introduced from equations 2 and 3, i.e.

early stage definition

$$\rho = \frac{2\pi r^4}{3m} E_{\phi} \quad [4]$$

late stage definition

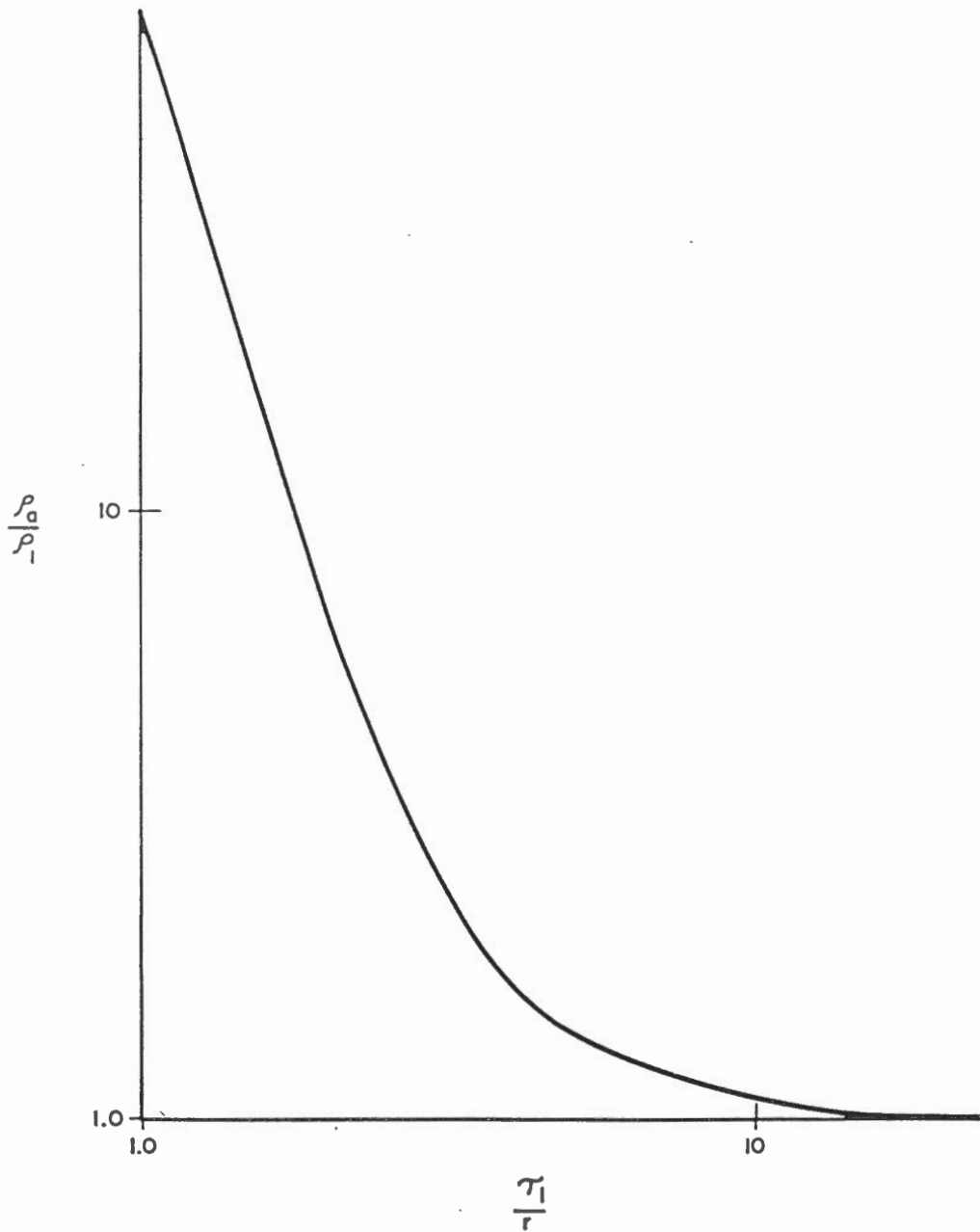
$$\rho = \frac{\mu}{4\pi t} \left(\frac{r\mu m}{5tE_{\phi}} \right)^{2/3} \quad [5]$$

For the present work it was found convenient to use the late stage expression for apparent resistivity. This is due to the fact that late stage behavior appears relatively quickly in the resistive onshore environments surveyed. Early stage behavior is only observed where near surface sediments are extremely conductive (offshore environments).

The interpretation of transient data mainly consists of comparing the measured apparent resistivity curves to curves computed for certain models of horizontally layered geoelectric sections. For this work, many theoretical apparent resistivity curves were calculated using specially developed computer programs. The algorithms of the computer programs are subject to the following assumptions:

- 1) the half-space is horizontally layered
- 2) the current in the transmitting dipole is a perfect step function

To understand the behavior of the apparent resistivity curves generated by using the definition of equation 5, consider the two examples given in Figures 5 and 6. Figure 5 is for homogeneous half-space of resistivity ρ_1 ; on the vertical axis is plotted the ratio of ρ_a/ρ_1 and on the horizontal axis the parameter τ_1/r . It can be seen that when $\tau_1/r > 10$, ρ_a/ρ_1 approaches 1, i.e. the apparent resistivity measured approaches the true resistivity of the half-space. In practice measurements are made at constant r . The true resistivity is measured when



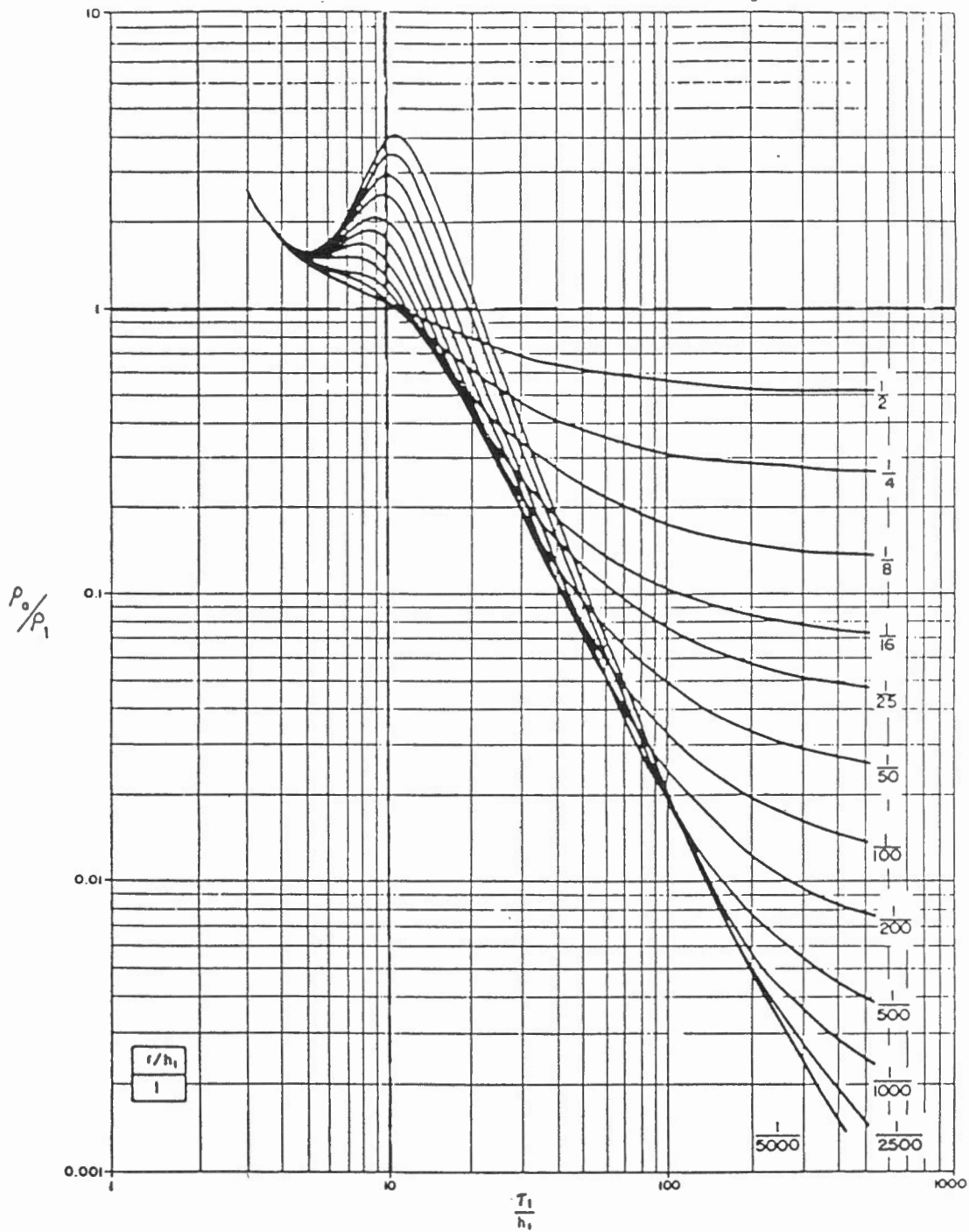
GEO-PHYSI-CON

ENGINEERING GEOPHYSICAL CONSULTANTS

MASTER CURVE
HOMOGENEOUS HALF-SPACE

C85-10

Figure 5



GEO-PHYSI-CON

ENGINEERING GEOPHYSICAL CONSULTANTS

MASTER CURVE
TWO-LAYER MEDIUM

C85-10

Figure 6

$$t > \frac{r^2}{2\pi\rho 10^5}$$

At values of $\tau/r < 10$, the values of ρ_a/ρ_1 can be seen to rapidly increase with decreasing τ/r . This is caused by the fact that the field, E_θ , at early time can no longer be described by the late stage asymptotic expression of equation 3. However, it can be expressed using the early stage asymptotic expression of equation 2.

Figure 6 shows late stage apparent resistivity curves for two layer sections when $\rho_2/\rho_1 < 1$. The resistivity stratification for the curves in Figure 6 could, for example, represent frozen ground underlain by unfrozen ground. On the horizontal axis, the parameter τ_1/h_1 is plotted, where h_1 is the thickness of the first layer (frozen ground). The main features of the apparent resistivity curves are:

- 1) At small values of the abscissa all curves merge into one corresponding to the behavior of uniform half-space of resistivity, ρ_1 .
- 2) At values of $8 < \tau_1/h_1 < 10$, the apparent resistivity curves for sections with $\rho_2/\rho_1 < 1/16$ and $r/h_1 \leq 1$ have a maximum.

- 3) At values of $\tau_1/h_1 > 10$, there are descending branches. For values of $\rho_2/\rho_1 < 1/16$ the descending branches have parallel segments.
- 4) At large values of τ_1/h_1 , the apparent resistivity curves approach ρ_2 .

4.1.2 Correction Factors for Ramp Time

It was stated in Section 4.1.1 that the master curves are computed for a perfect step function. The transmitter current when turned off has a finite ramp time (Section 4.1). To make the measured apparent resistivity curve correspond to the master curves a correction must be made for the ramp turn-off. The correction factors that are often used are based on either the late stage behavior of the field or the full expression of the field for a homogeneous half-space. In resistive environments (on shore) the late stage expression for the correction is used, as it is valid over most of the time range employed. In conductive environments (off shore) the correction based on the full field expression is used, as late stage appears more slowly.

The late stage correction factors are based on the fact that, at late time, the field is proportional to $t^{-5/2}$, so that

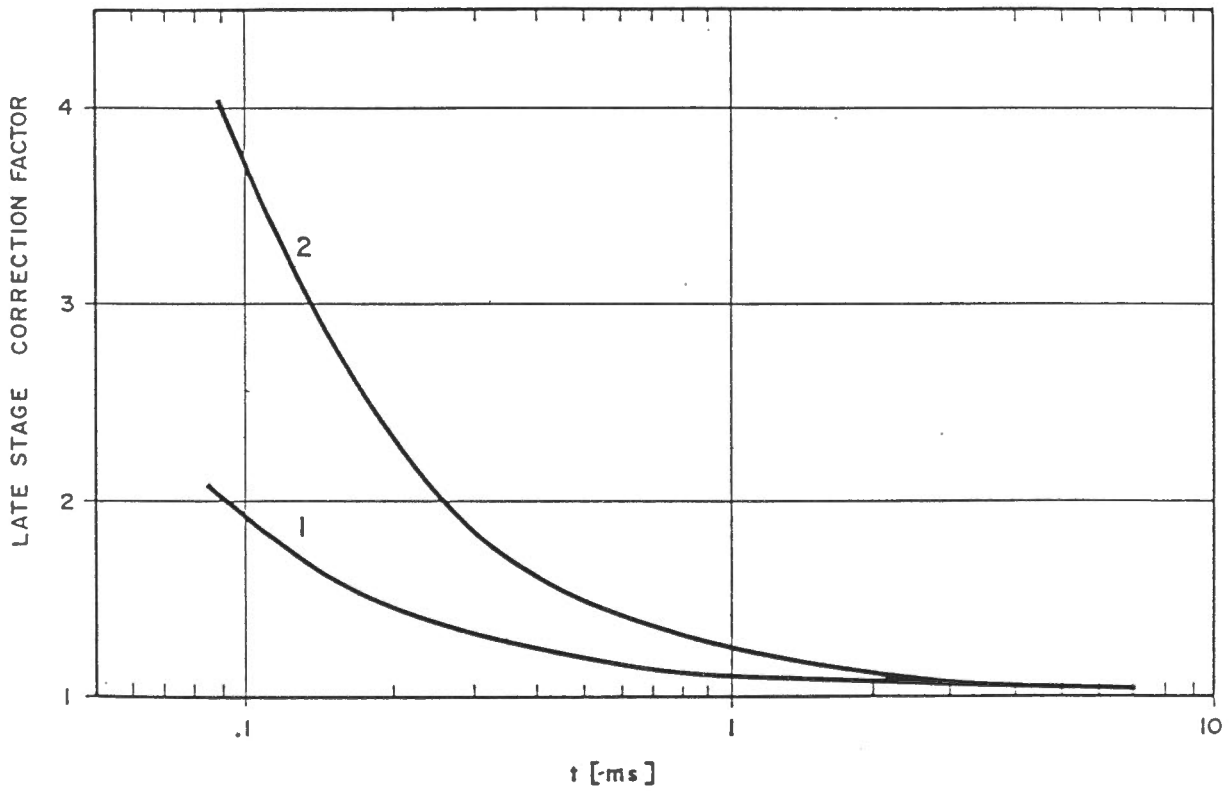
$$\frac{Q(t)}{R(t)} = \frac{1}{\Delta T} \int_t^{t+\Delta T} t^{-5/2} dt \quad [6]$$

where $Q(t)$ is the field due to the linear ramp at a time, t ,
 ΔT is the ramp time, and
 $R(t)$ is the field measured due to a perfect step function at time, t

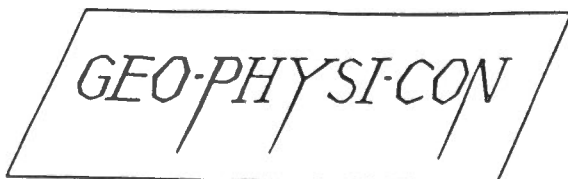
The full expression correction factor is based on the relation:

$$E_{\theta} = \frac{3m\rho}{2\pi r^4} \left[\vartheta(u) - \sqrt{\frac{2}{\pi}} u \left(1 + \frac{u^2}{3} \right) e^{-u^2/2} \right] \quad [7]$$

where the parameter $u = 2\pi r/\tau$,
 $\vartheta(u)$ is the error function
 τ is $\sqrt{2\pi\rho t 10^7}$,
 m is the transmitter dipole moment, and
 ρ is the half-space resistivity.



- 1 Ramp time 70 microsec
- 2 Ramp time 200 microsec



ENGINEERING GEOPHYSICAL CONSULTANTS

CORRECTION FOR RAMP TIME

C 85-10

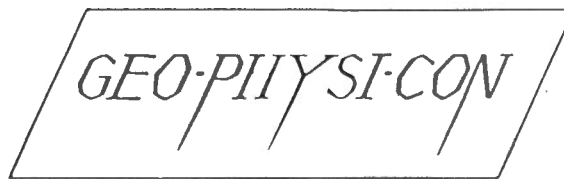
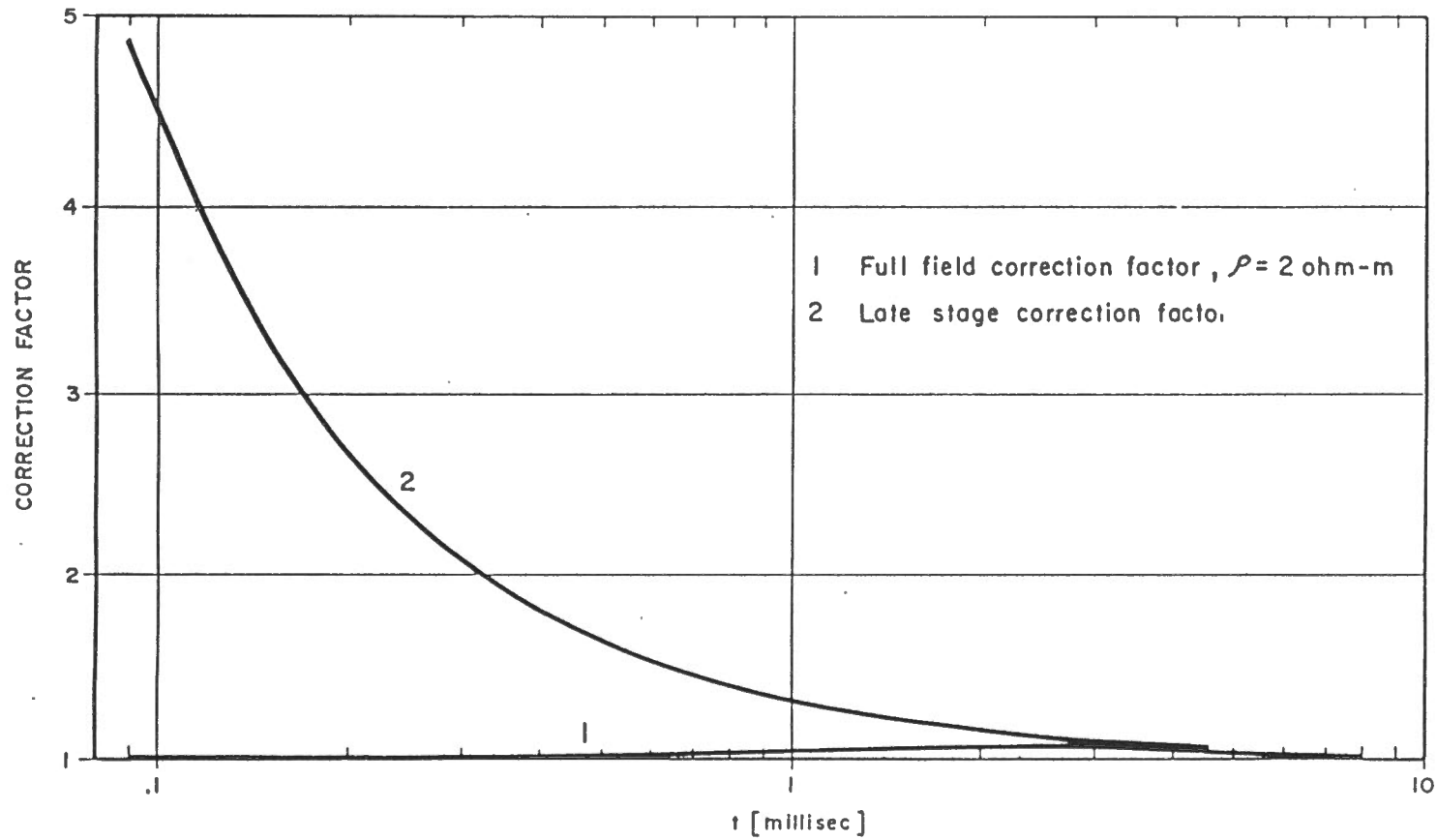
Figure 7

In Figure 7 the late stage correction factor is plotted as a function of t for two values of ΔT . In Figure 8 the correction factor based on late stage and on the full expression for the field for a homogeneous half-space having a resistivity of 2 ohm-m are compared. In Figure 9, the difference in apparent resistivities, using the two different correction factors, is shown. The curves merge at the onset of late stage behavior.

4.1.3 Influence of Turn-On Time and Ramp Time of Previous Pulse

The current waveform in the transmitter loop, as discussed in Section 4.1, consists of periods of time-on and time-off. The electromotive force in the receiver is measured only during time-off. The master curves are computed on the assumption that the secondary field is induced by the last ramp turn-off only. It is assumed that the secondary field, due to previous changes in current, has decayed to a negligible level.

It had been previously found that under certain conditions the turn-on time and ramp turn-off of a previous pulse can influence the measured secondary field.

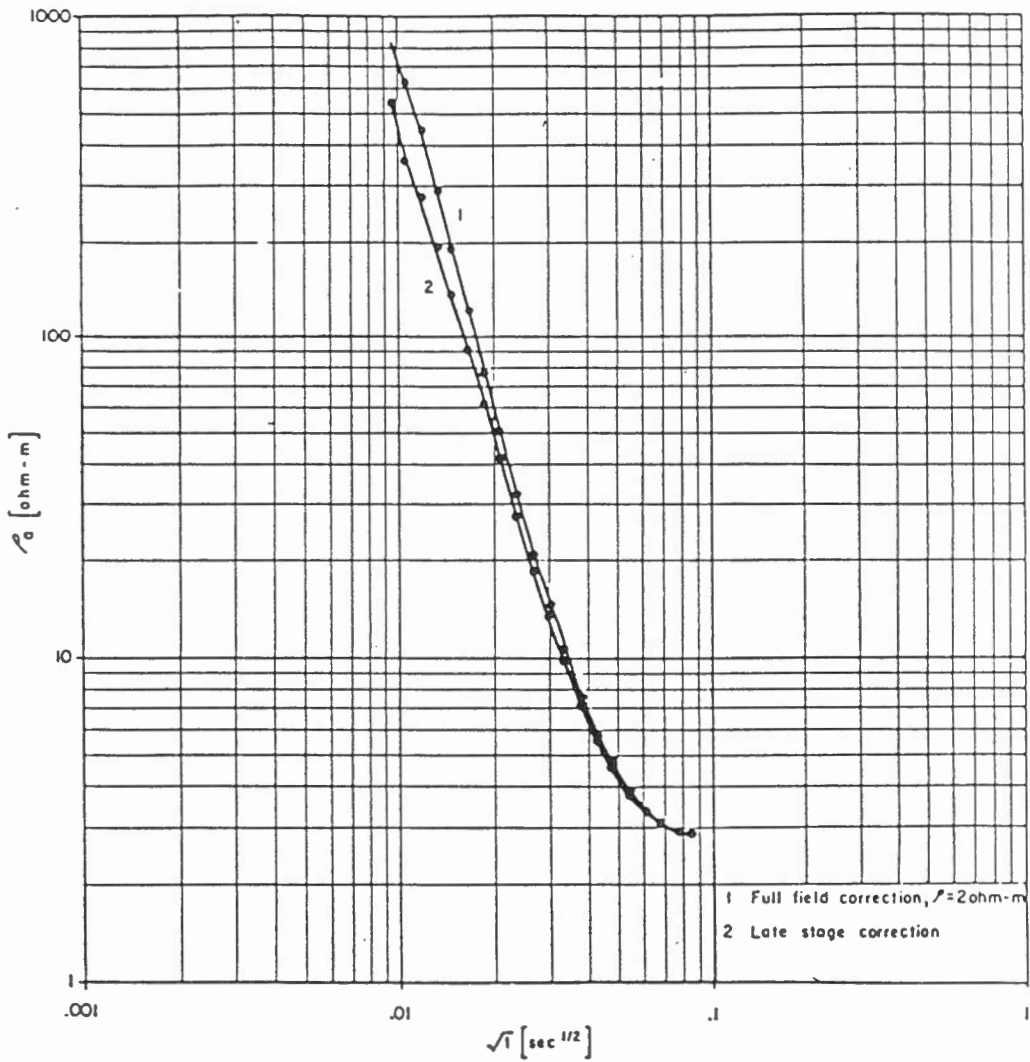


ENGINEERING GEOPHYSICAL CONSULTANTS

CORRECTION FACTORS
 FOR RAMP TIME (250 microsec)

C 85-10

Figure 8



GEO-PHYSI-CON

ENGINEERING GEOPHYSICAL CONSULTANTS

APPARENT RESISTIVITY CURVES
WITH DIFFERENT CORRECTION

C 85-10

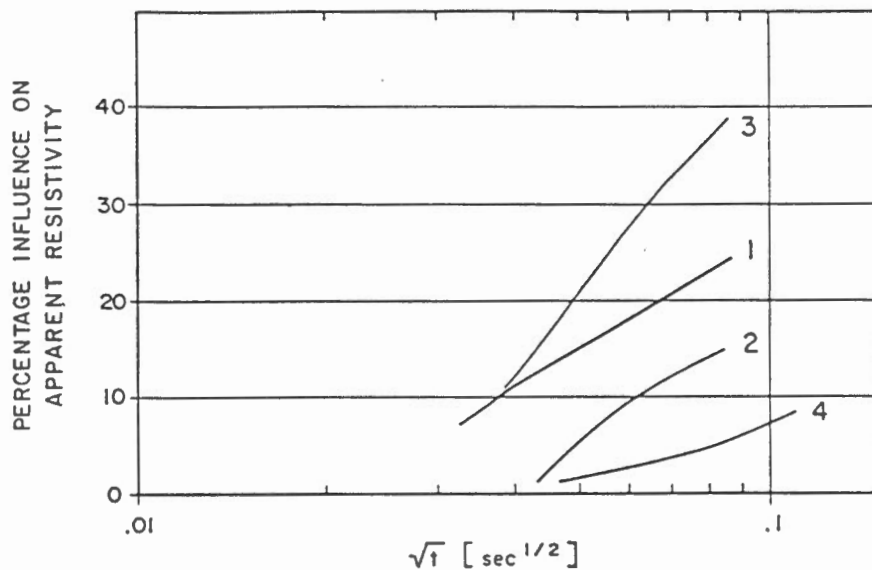
Figure 9

In Figure 10 the influence of the turn-on pulse on the apparent resistivity is computed from master curves for the geoelectric sections typical for onshore permafrost. The computations are made for high and low frequencies. The effect of pulse turn-on can be reduced by measurements at a lower frequency in the same time range, since the last ten time channels at a higher frequency are equivalent to the first 10 time channels at the lower frequency.

4.2 EM31 and EM34-3 - Fixed Frequency Systems

In the EM method eddy current flow is induced in the ground by the time varying magnetic field of a vertical or horizontal magnetic dipole transmitter operating at a fixed frequency. The eddy current flow induces a secondary magnetic field which, together with the primary field, is sensed by a similar receiver dipole. The ratio of the primary and secondary fields is related to the conductivity of the subsurface.

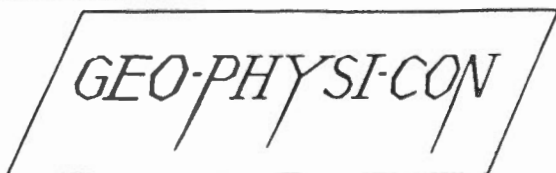
The instrument parameters, frequency and coil separation, are selected so that operation can be described by the low induction number approximation. In this sense each induced eddy current loop is independent of the others and the measured



ρ_1	h_1	ρ_2	h_2	ρ_3	h_3	ρ_4	h_4	ρ_5
150	50	1000	200	200	150	1000	400	2.5

LEGEND

- 1 Turn-on time for HF
- 2 Previous turn-off time for HF
- 3 Sum of 1 and 2
- 4 Turn-on time for LF



ENGINEERING GEOPHYSICAL CONSULTANTS

INFLUENCE OF SUPERPOSITION OF
PULSES FOR
ON-SHORE GEOELECTRIC SECTION

C85-10

Figure 10

(apparent) conductivity can be thought of as a linear superposition of the responses of strata within the exploration range of the array used.

Under certain restrictions concerning the maximum value of terrain conductivity the measured and strata conductivities are related by the following expression:

$$\sigma_a = \sum_{i=1}^n \sigma_i (R_i - R_{i-1}) \quad [8]$$

where σ_a is the apparent conductivity
 σ_i is the conductivity of the i th layer, and
 R_i, R_{i-1} are geometric (weighting) factors characteristic of the top and bottom of the i th layer

The effective exploration depth of the EM equipment can be varied by changing one or more of loop spacing(s), loop orientation (vertical or horizontal), or height above terrain (h_0). All these parameters affect the distribution of the geometric factors. For horizontal coplanar loops geometric factors are described by

$$R(D) = (D^2 + 1)^{-1/2} \quad [9]$$

and for vertical coplanar loops

$$R(D) = [(D^2 + 1)^{1/2} - D] \quad [10]$$

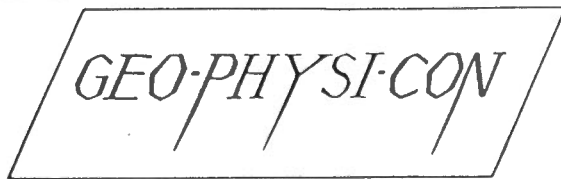
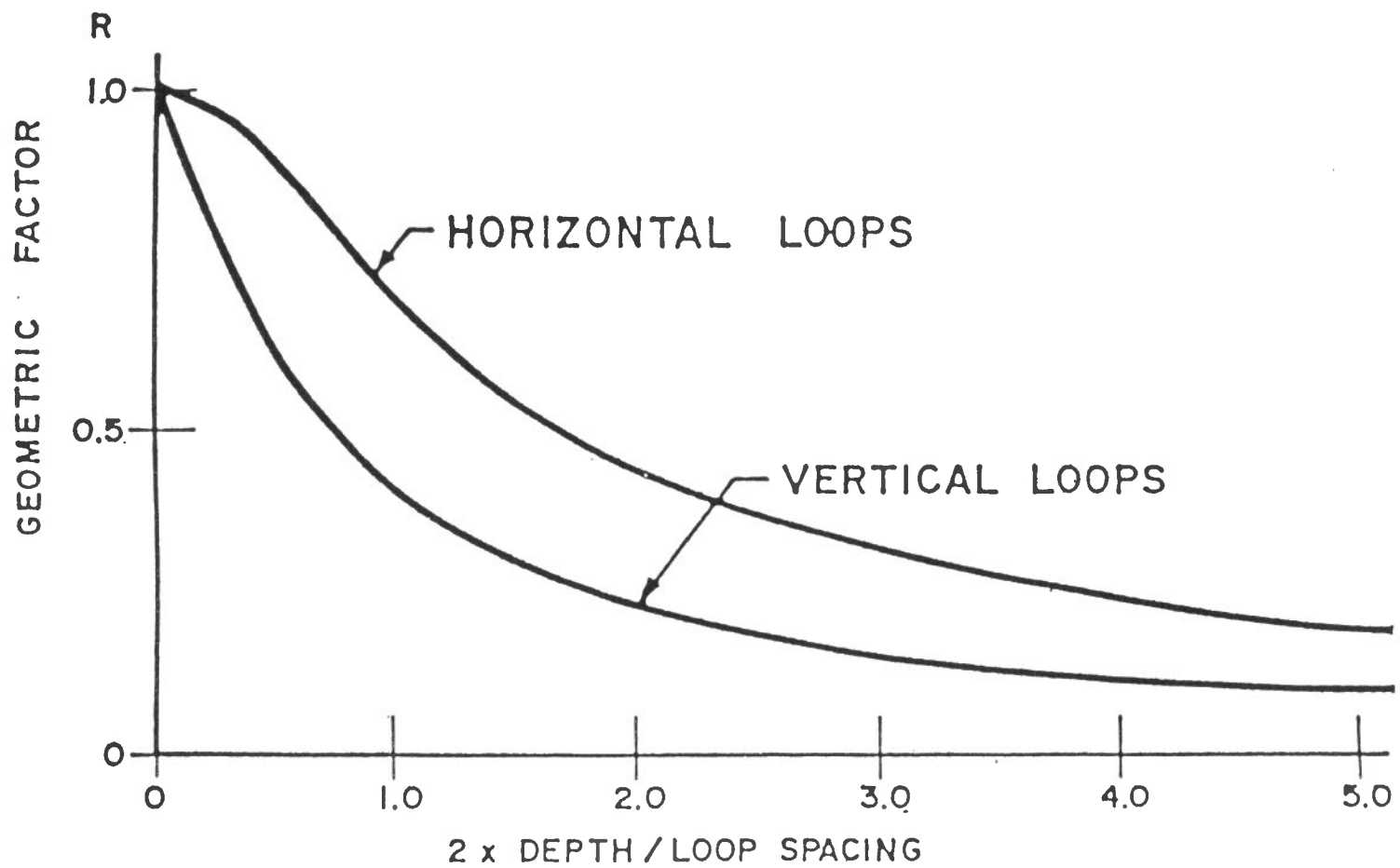
where the parameter $D = 2(h_0 + d)/s$ [11]

and d is the depth below ground surface

A graph of the functions [9] and [10], above, is shown in Figure 11. From this figure it is evident that, for a common loop spacing, the horizontal loop mode senses effectively twice as deep as the vertical loop mode. The units of apparent conductivity used in this work are millimhos/metre. For the TEM method the units for apparent resistivity are ohm-metres. These are related by

$$(\text{mmho/m}) = (\text{ohm-m})^{-1} \times 10^3$$

Detailed manufacturer's specifications for the instruments used are given in Appendix A.



ENGINEERING GEOPHYSICAL CONSULTANTS

GEOMETRIC FACTORS FOR
HORIZONTAL AND VERTICAL LOOPS

C 85-10

Figure 11

5.0 BASIC PRINCIPLES OF USE OF INFORMATION ON PERMAFROST DISTRIBUTION FROM TEM DATA FOR CDP STATIC CORRECTION

Numerous results of laboratory and in-situ measurements show that both electrical resistivities and acoustic velocities vary with temperature. It has been found that electrical and elastic properties of frozen material demonstrate similar behavior as a function of temperature, ice content, lithology, etc. This similarity creates a basis for using the information on permafrost obtained by electrical methods for reflection seismic data processing to make a reliable correction for permafrost influence.

Previous electrical surveys for delineation of frozen material in the subsurface have shown that

- 1) permafrost distribution in the Canadian Arctic can be very complex
- 2) the information on permafrost distribution from electrical methods is in good agreement with crystal cable velocity log data.

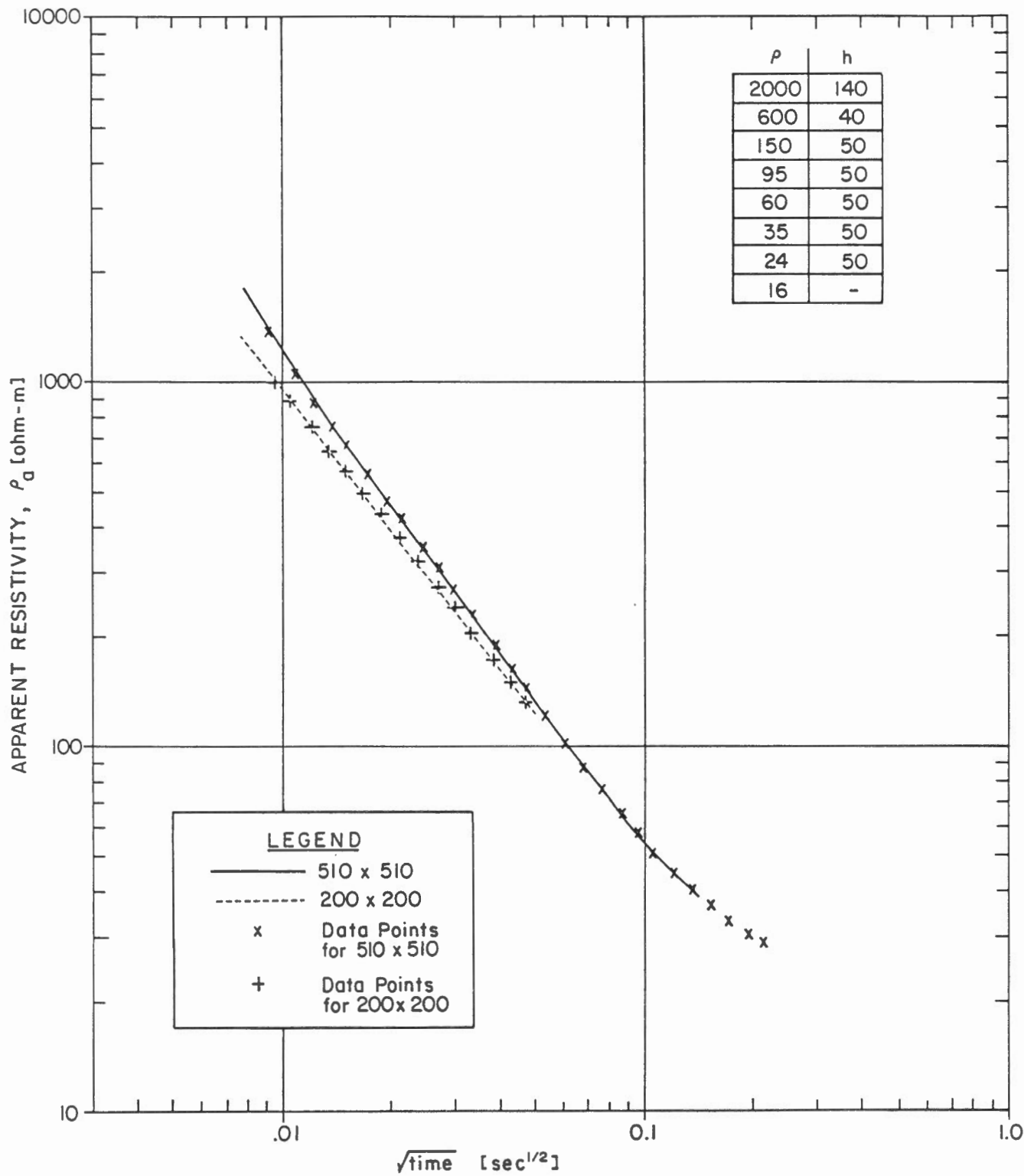
The paper included in Appendix B provides more details on this subject.

6.0 RESULTS

The interpretation of transient data was performed by comparison of measured and modelled apparent resistivity curves. This procedure is described in detail in previous reports (1, 2, 3).

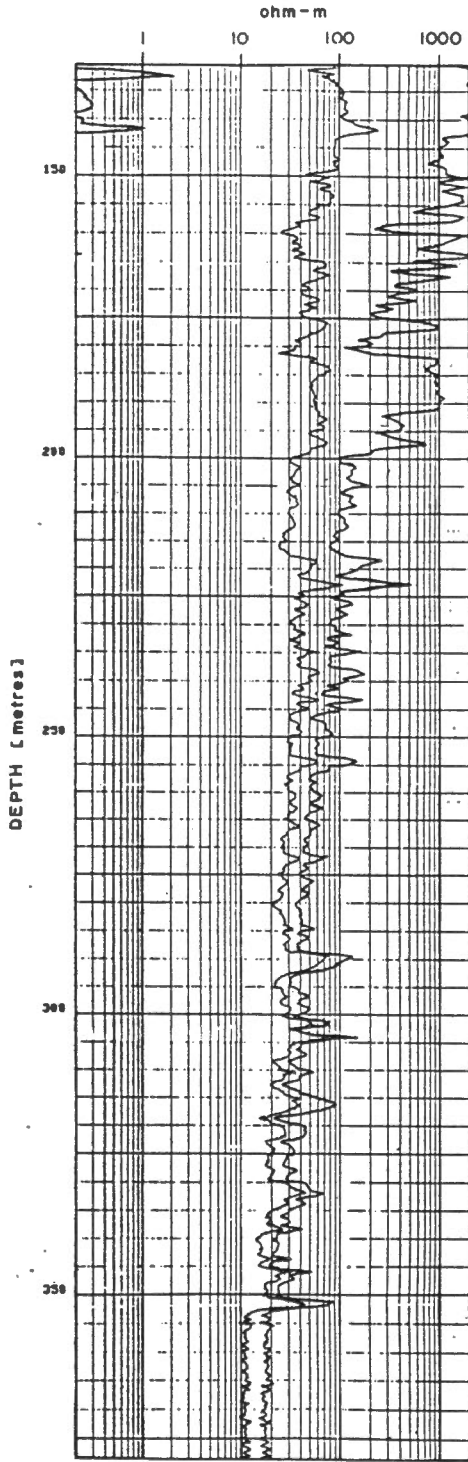
6.1 Geoelectric Structure

Figure 12 gives an example of model curves with superimposed data points for the transmitter loop sizes used. There are two major zones in the interpreted section. The first zone has a net thickness of 180 m and consists of two layers: 2000 ohm-m and 600 ohm-m. It corresponds to the upper, most resistive portion of the frozen section. The second zone is comprised of a number of layers of equal thickness. The resistivity of the layers decreases with depth by a factor of, approximately 1.6. This set of layers simulates a gradual decrease of resistivity with depth which is confirmed by the resistivity logs from wells in the vicinity of the survey line (Figure 13). These gradual changes are expected to be due primarily to variations in temperature and/or ice content.



GEO-PHYSI-CON

TEM MEASURED
AND MODELLED CURVES
STATION I



GEO-PHYSI-CON

RESISTIVITY LOG

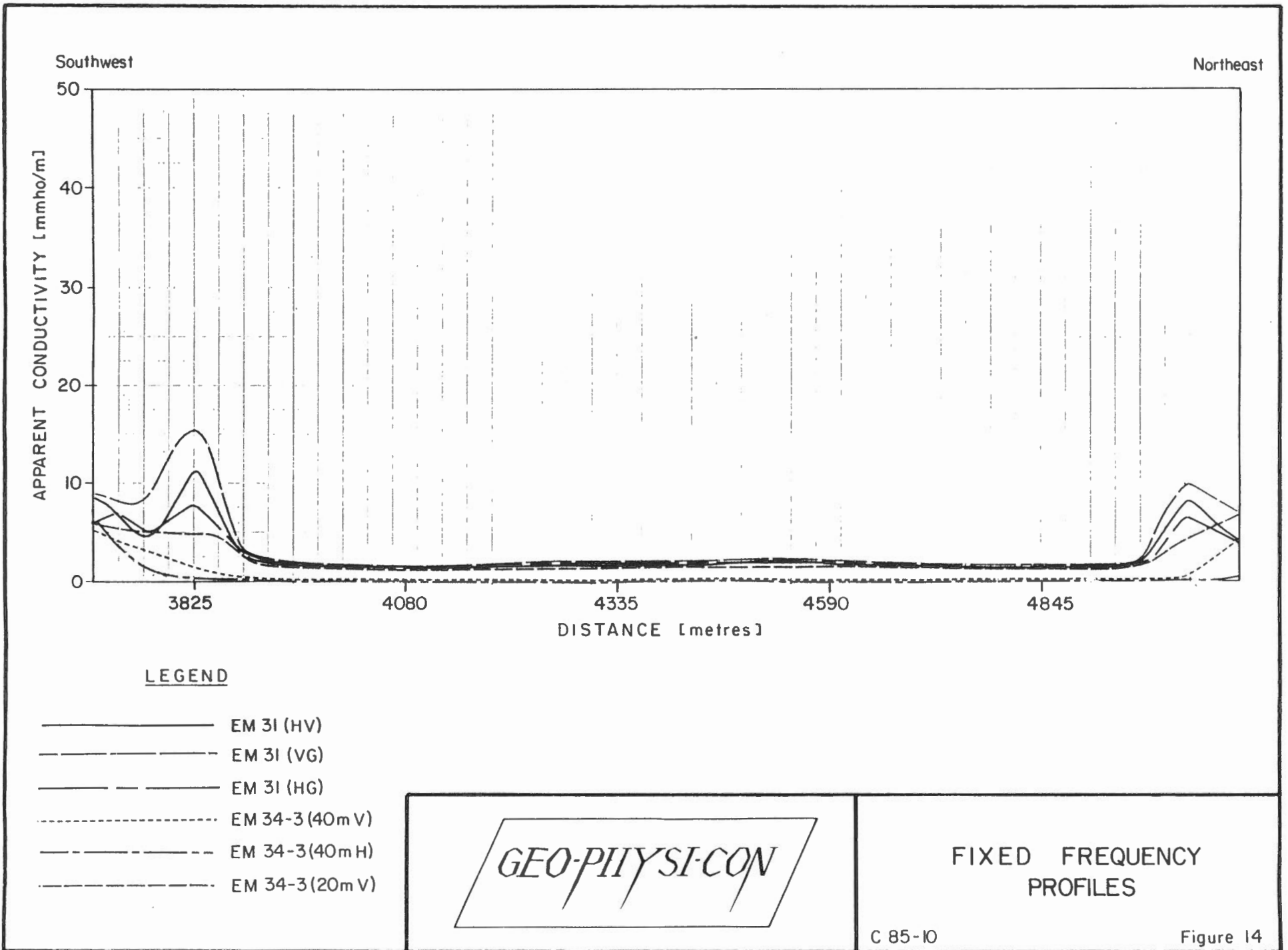
A drastic change in resistivity occurs at the boundary separating the zones. In the further discussion this interface will be referred to as the "major boundary".

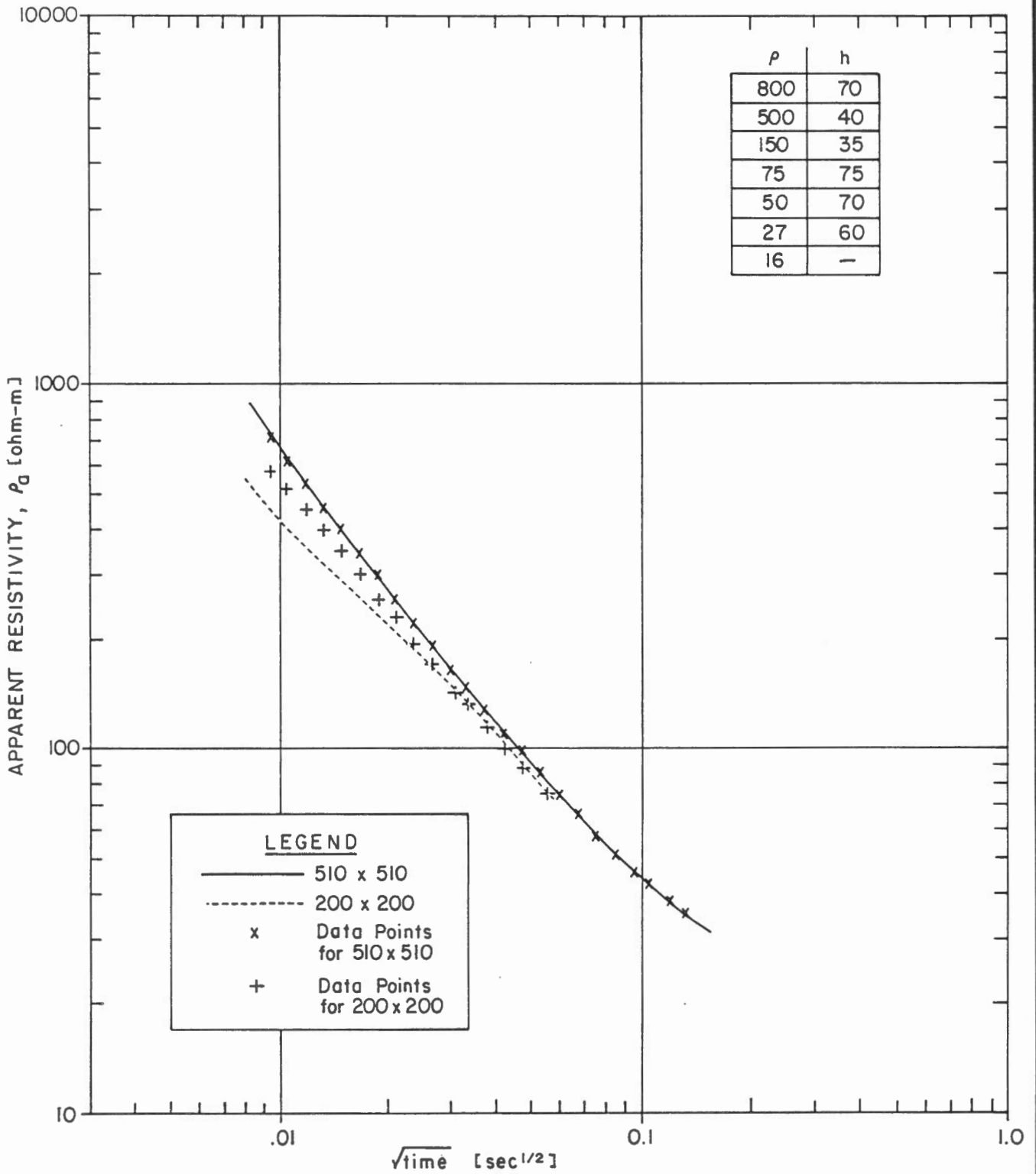
6.2 EM Data

Figure 14 gives an example of fixed frequency profiles. The profiles show a very high resistivity (greater than 1000 ohm) to the depth of a least 40 m. This is in a good agreement with both TEM data and resistivity logs available. The increase in conductivity at the southern and northern ends corresponds to the presence of lakes.

6.3 Distortion of Apparent Resistivity Curves

Figure 15 gives another example of measured apparent resistivities superimposed onto model curves. It is obvious that the large loop data points are in a good agreement with the model curves while the small loop data points deviate at earlier time gates. The reason for this deviation is the influence of lateral changes in shallow resistivity. At later time the measured and model curves tend to merge which illustrates more homogeneous distribution of resistivity at greater depth.





GEO-PHYSI-CON

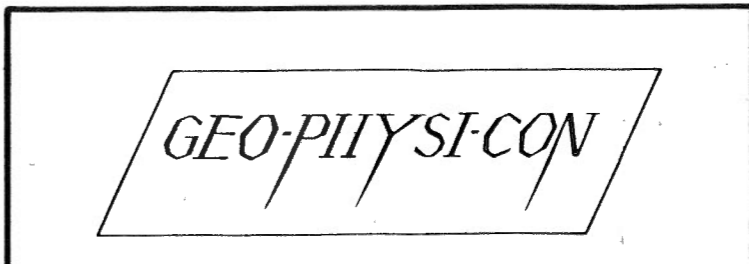
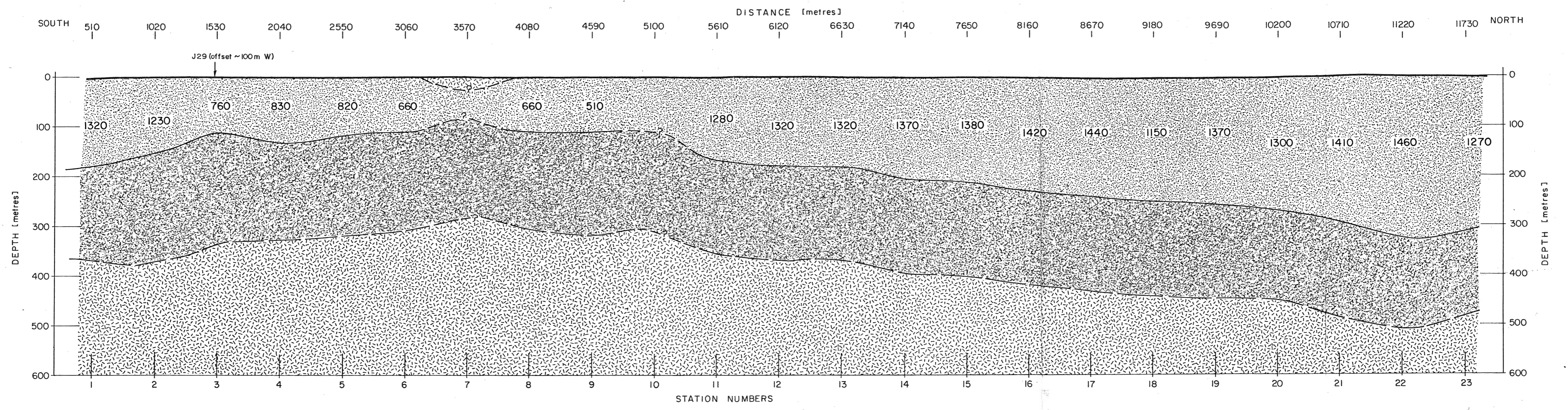
TEM MEASURED
AND MODELLED CURVES
STATION 8

6.4 Interpreted Section

Figure 16 shows the resulting interpreted section. Two boundaries are present. The upper one is the major boundary and corresponds to the top of the zone of gradual decrease in resistivity. The depth to the major boundary is about 200 m at the southern end of the survey line, about 100 m between stations 7 and 10, and then increases to over 300 m to the northern end.

The numbers above the major boundary represent the average resistivities for the upper zone. It has been found from both laboratory and in-situ measurements that changes in resistivity of frozen sediments correlate to similar changes in elastic properties (see Appendix B). Therefore, the variations in resistivity detected by the TEM method can be expected to manifest themselves on the reflection seismic time sections.

The lower boundary outlines the base of permafrost. It is most probable that there is no clear permafrost bottom but, rather, the transition from frozen ground to unfrozen ground occurs gradually, following changes in temperature and fraction of frozen water.



INTERPRETED SECTION

C 85-10

Figure 16

A value of 30 ohm-m has been selected as a representative value for the base of permafrost. This boundary has approximately the same shape as the major boundary. The depth of occurrence varies from 380 m at the southern end, decreases to less than 300 m between stations 7 and 10 and exceeds 500 m at the northern end.

It should be noted that varying the resistivity of 30 ohm-m selected for the permafrost base would not change the shape of this boundary. This would also not greatly affect the depth of its occurrence.

7.0 CONCLUSIONS

The results presented show that the objectives of the first stage of the test program were met. The TEM method was successfully employed for mapping the distribution of the frozen material in the subsurface. The main features of the frozen section detected by the TEM method are listed below.

- 1) Two major zones were discovered within the frozen section.

GEO-PHYSI-CON

- 2) The upper zone consists of two layers over most of the survey line. The average resistivity of this zone changes along the survey line. These changes in electrical properties are expected to correlate to similar changes in acoustic velocity and, accordingly, to affect seismic time sections.

- 3) Gradual decrease of resistivity with depth was interpreted to take place within the lower zone. The decrease is expected to be due to variations in temperature and ice content. Due to the gradual changes it is problematic to determine the base of ice bearing permafrost by any geophysical method or using temperature measurements. However, there are all reasons to expect that elastic properties at the base of permafrost would vary in the similar gradual manner. The shape of the permafrost base detected with selected resistivity of 30 ohm-m is expected to be reasonably well defined.

- 4) Both the major boundary and the base of permafrost are not horizontal and have an apparent arch-type structure. This is also expected to affect the seismic time sections.

8.0 RECOMMENDATIONS

Regarding the subsequent stages of the test program the following recommendations can be made:

- 1) The analysis of electrical and acoustic logs, temperature measurements etc. both available in literature and obtained during recent surveys would provide valuable information for the next stages of the test program.
- 2) It appears to be beneficial to have a Geo-Physi-Con representative involved at the following stages of the test program to combine the electrical and seismic data in the most efficient manner.


Planning similar surveys in the future the following additional surface techniques can be recommended.


- 1) The use of shallow high resolution reflection seismic survey would be of substantial help in transforming the permafrost depth section into a seismic time section.


GEO-PHYSI-CON

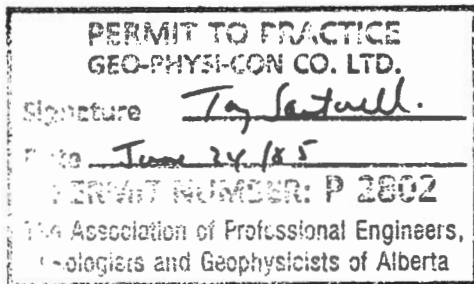
- 2) DC sounding method can provide valuable information on near surface resistivity.

Respectfully submitted,
GEO-PHYSI-CON CO. LTD.,

Per: 
Grigory Rozenberg, M.Sc.
Senior Geophysicist

Per: 
J. D. Henderson
President

Reviewed by: 
T. Sartorelli, P.Eng.,
Vice-President
Senior Geophysicist



Calgary, Alberta
June 1985
C85-10

REFERENCES

1. "Detection of Permafrost Base in Thick Permafrost Areas, Transient Electromagnetic Survey, MacKenzie Delta Area, N.W.T." Report prepared for Energy, Mines and Resources, Earth Physics Branch, Division of Gravity, Geothermal and Geodynamics, June 1983.
2. "TEM Survey to Map the Distribution of Permafrost, Drake Point, Melville Island, N.W.T." Report prepared for Dept. of Energy, Mines & Resources, Earth Physics Branch, June 1983.
3. "Transient Electromagnetic Survey, Permafrost Structure Mapping,, Tuktoyaktuk Area, N.W.T." Report prepared for Energy, Mines and Resources, Geological Survey of Canada, Resource Geophysics and Geochemistry Division, May 1983.



TERRAIN CONDUCTIVITY METERS

ONE MAN - CONTINUOUS READING



EM31

The Geonics EM31 provides a measurement of terrain conductivity without contacting the ground using a patented inductive electromagnetic technique. The instrument is direct reading in millimhos per meter and surveys are carried out simply by traversing the ground.

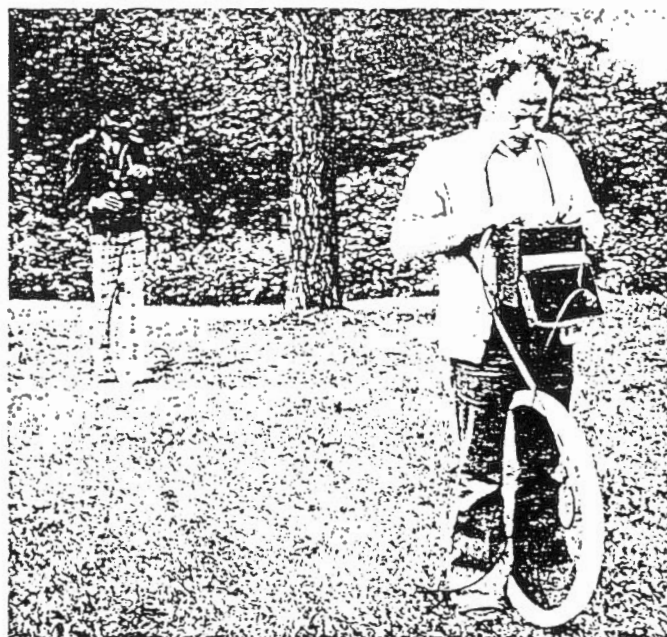
The effective depth of exploration is approximately six meters making it ideal for engineering geophysics. By eliminating ground contact, measurements are easily carried out in regions of high resistivity such as gravel, permafrost and bedrock. Over a uniform half space the EM31 reads identically with conventional resistivity and the measurement is analogous to a conventional galvanic resistivity survey with a fixed array spacing. Interpretation curves supplied with each instrument often permit an estimate of a layered earth.

The advantages of the EM31 are the speed with which surveys can be carried out, the ability to precisely measure small changes in conductivity, and the continuous readout which provides a previously unobtainable lateral resolution.

Specifications

MEASURED QUANTITY	Apparent conductivity of the ground in millimhos per meter.
PRIMARY FIELD SOURCE	Self-contained dipole transmitter
SENSOR	Self-contained dipole receiver
INTERCOIL SPACING	3.66 meters
OPERATING FREQUENCY	9.8 kHz
POWER SUPPLY	8 disposable alkaline 'C' cells (approx. 20 hrs life continuous use)
CONDUCTIVITY RANGES	3, 10, 30, 100, 300, 1000 mmhos/meter
MEASUREMENT PRECISION	±2% of full scale
MEASUREMENT ACCURACY	±5% at 20 millimhos per meter
NOISE LEVEL	<0.1 millimhos per meter
OPERATOR CONTROLS	<ul style="list-style-type: none">● Mode Switch● Conductivity Range Switch● Phasing Potentiometer● Coarse Inphase Compensation● Fine Inphase Compensation
DIMENSIONS	Boom : 4.0 meters extended 1.4 meters stored Console : 24 x 20 x 18 cm Shipping Crate : 155 x 42 x 28 cm
WEIGHT	Instrument Weight : 9 kgm Shipping Weight : 23 kgm

TWO MAN - VARIABLE DEPTH



EM34-3

Operating on the same principles as the EM31, the EM34-3 is designed to achieve a substantially increased depth of exploration and a readily available vertical conductivity profile.

The underlying principle of operation of this patented non-contacting method of measuring terrain conductivity is that the depth of penetration is independent of terrain conductivity and is determined solely by the instrument geometry i.e. the intercoil spacing and coil orientation. The EM34-3 can be used at three fixed spacings of 10, 20, or 40 meters and in the vertical coplanar (as shown) or horizontal coplanar mode. In the vertical coplanar mode, the instrument senses to approx. 0.75 of the intercoil spacing. In the horizontal coplanar mode, the instrument can sense to 1.5 times the intercoil spacing. For the horizontal coplanar mode, however, coil misalignment errors are more serious than in the vertical mode so greater care must be exercised to achieve the maximum 60 meter depth.

Simple operation, survey speed and straight forward data interpretation makes the EM34-3 a versatile and cost effective tool for the engineering geophysicist.

Specifications

MEASURED QUANTITY	Apparent conductivity of the ground in millimhos per meter
PRIMARY FIELD SOURCE	Self-contained dipole transmitter
SENSOR	Self-contained dipole receiver
REFERENCE CABLE	Lightweight, 2 wire shielded cable
INTERCOIL SPACING & OPERATING FREQUENCY	<ul style="list-style-type: none">● 10 meters at 6.4 kHz● 20 meters at 1.6 kHz● 40 meters at 0.4 kHz
POWER SUPPLY	Transmitter : 8 disposable 'D' cells Receiver : 8 disposable 'C' cells
CONDUCTIVITY RANGES	3, 10, 30, 100, 300 mmhos/meter
MEASUREMENT PRECISION	±2% of full scale deflection
MEASUREMENT ACCURACY	±5% at 20 millimhos per meter
NOISE LEVEL	<0.2 millimhos per meter
DIMENSIONS	Receiver Console : 19.5 x 13.5 x 26cm Transmitter Console : 15 x 8 x 26cm Coils : 63cm diameter
WEIGHTS	Receiver Console : 3.1 kg Receiver Coil : 3.2 kg Transmitter Console : 3.0 kg Transmitter Coil : 6.0 kg Shipping Weight : 41. kg

EM37 Ground Transient Electromagnetic System
Technical Specifications

Transmitter

- Current Waveform - See Fig.A1
- Repetition rate - 3Hz or 30Hz in countries using 60Hz power line frequency; 2.5Hz or 25Hz in countries using 50Hz power line frequency; all four base frequencies are switch selectable.
- Turn-off time (Δt) - fast linear turn-off of maximum 300 μ sec. at 20 amps into 300x600m loop. Decreases proportionally with current and (loop area)^{1/2} to minimum of 20 μ sec. Actual value of Δt read on front panel meter.
- Transmitter loop - any dimensions from 40x40m to 300x600m maximum at 20 amps. Larger dimensions at reduced current. Transmitter output voltage switch adjustable for smaller loops. Value of loop resistance read from front panel meter; resistance must be greater than 1 ohm on lowest voltage setting to prevent overload.
- Transmitter protection - circuit breaker protection against input over-voltage; instantaneous solid state protection against output short circuit; automatically reset on removal of short circuit. Input voltage, output voltage and current indicated on front panel meter.
- Transmitter output voltage - 150 volts (zero to peak) maximum; 20 volts (zero to peak) minimum
- Transmitter output power - 2.8 kw maximum
- Transmitter wire supplied - 1800m. #10 copper wire PVC insulated with nylon jacket; transmitter wire contained on 6 reels (supplied); 2 reel winders supplied.
- Transmitter motor generator - 5 HP Honda gasoline engine coupled to 120 volt, 3 phase, 400Hz alternator. Approximately 8 hours continuous operation from full (built-in) fuel tank.

Receiver

- Measured quantity - time rate of decay of magnetic flux along 3 axes.
- Sensors - two air cored coils of bandwidths 11 and 50 kHz respectively; each 66cm dia.x4x5cm cross-section. Low frequency coil for general use, high frequency coil for shallow sounding.
- Time channels - 20 time channels with locations and widths as shown in Fig.A2. Successive operation at 30Hz, then 3Hz, effectively gives 30 channels covering range from 80 μ sec. to 80 msec.
- Output display - 4 figure digital LED plus sign; display also shows channel number and gain.
- Integration time - 2^n cycles at 30Hz; n=4,6,8,10,12,14 (switch selectable); similar integration times at other base frequencies.
- Receiver noise - approximately 1.5×10^{-10} volt/m²/turn of receiver coil at last gate at 30Hz with integration time of 34 seconds. Noise will be higher during intense local spherics activity.
- Output connector - all 20 channels available in analogue format from output connector at 5 volts fsd level.
- Synchronization to Tx - any of the following (switch selectable)
(1) reference cable
(2) primary pulse
(3) 27 MHz radio link (40 channels)
(4) high stability (oven controlled) quartz crystals
- Noise rejection circuitry - with any of (1)-(3) above, entire system is automatically synchronized to 50/60Hz power line frequency when such interference exists in survey area; selective clipping of atmospheric noise pulses at all times. Audio output of Rx coil (transmitter pulse blanked out) is available on built-in loud speaker for ready identification of interference.
- Receiver batteries - 12 volt rechargeable Gel-cells; either 9 hours continuous operating time at 17°C (battery weight

Receiver - Cont'd

Receiver batteries (continued) - battery weight 7.6 kg, 20 amp hour) or 2.5 hours continuous operating time (battery weight 2.6 kg, 6 amp hour). Two sets of batteries and a battery charger supplied to permit charging of spare set from transmitter motor-generator during survey.

Special Report 85-5

May 1985



US Army Corps
of Engineers

Cold Regions Research &
Engineering Laboratory

Workshop on permafrost geophysics *Golden, Colorado, 23-24 October 1984*

J. Brown, M.C. Metz and P. Hoekstra, Editors



Prepared in cooperation with
COMMITTEE ON PERMAFROST
POLAR RESEARCH BOARD
NATIONAL RESEARCH COUNCIL
WASHINGTON, D.C.

Special Report 85-5

WORKSHOP ON PERMAFROST GEOPHYSICS

Golden, Colorado, 23-24 October 1984

Edited by

J. Brown
M.C. Metz
P. Hoekstra

May 1985

Prepared in cooperation with
Committee on Permafrost, Polar Research Board
National Research Council, Washington, D.C.

by

U.S. Army Cold Regions Research and Engineering Laboratory
Hanover, New Hampshire

SOME ASPECTS OF TRANSIENT ELECTROMAGNETIC SOUNDINGS
FOR PERMAFROST DELINEATION

G. Rozenberg, J.D. Henderson and A.N. Sartorelli
Geo-Physi-Con Co. Ltd.
Calgary, Alberta, Canada

A. Judge
Department of Energy, Mines and Resources
Ottawa, Ontario, Canada

INTRODUCTION

A variety of geophysical methods have been applied over the last few decades to map the top and bottom of permafrost. A good review of different geophysical techniques for permafrost investigation and a representative bibliography may be found in Scott et al. (1978). Among more recent papers, Hatlelid and MacDonald (1982) and Sartorelli and French (1982) can be recommended.

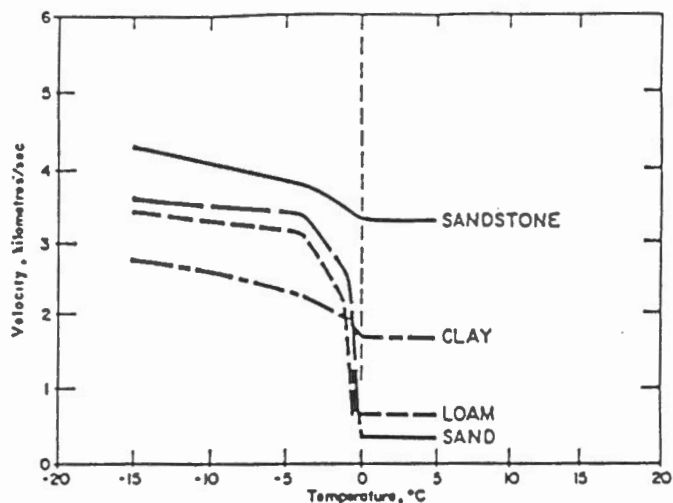
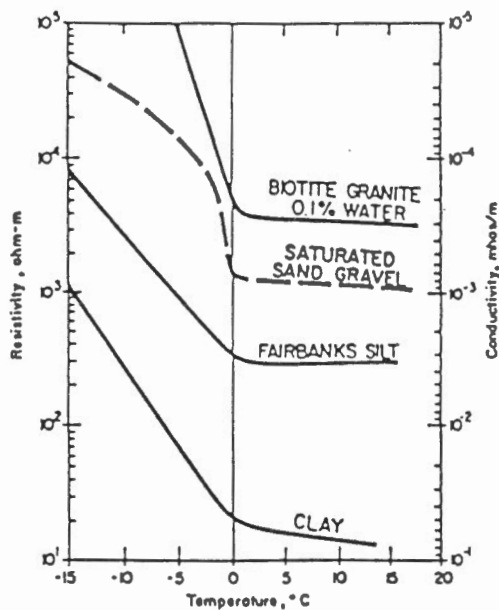
During the past three years, the method of transient electromagnetic (TEM) soundings has been successfully employed to delineate upper and lower permafrost surfaces in a number of arctic areas. Kaufman and Keller (1983) describe the theoretical basis of the method. Rozenberg and Hoekstra (1982) and Ehrenbard et al. (1983) describe the characteristics of the method which make it suitable for permafrost investigations and present case histories for surveys performed in the vicinity of the Alaskan Beaufort coast.

This paper illustrates the use of the TEM method for permafrost mapping under more complex conditions. Three of the four cases cited are taken from surveys in the western Canadian Arctic.

GENERAL PRINCIPLES

The physical basis for the delineation of permafrost using geophysical methods lies in the fact that the physical properties of subsurface materials vary with temperature. Figure 1 illustrates typical dependencies of electrical resistivity and velocity of compression waves on temperature and lithology. It is apparent that both electrical resistivity and compression wave velocity are similarly affected by temperature and tend to increase as temperature decreases for different lithologies.

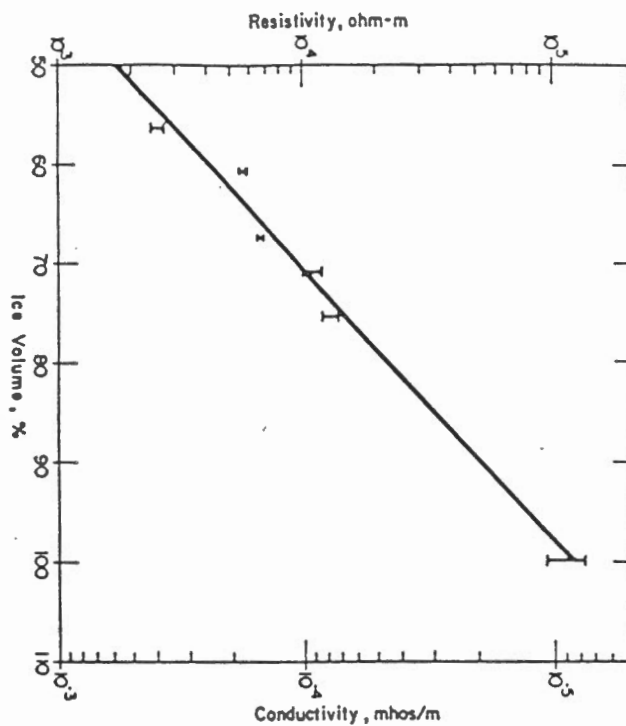
Figure 2 shows the variations in resistivity and seismic velocity as ice content changes. Again the similarity is obvious.



a. Conductivity vs temperature (Hoekstra et al. 1975).

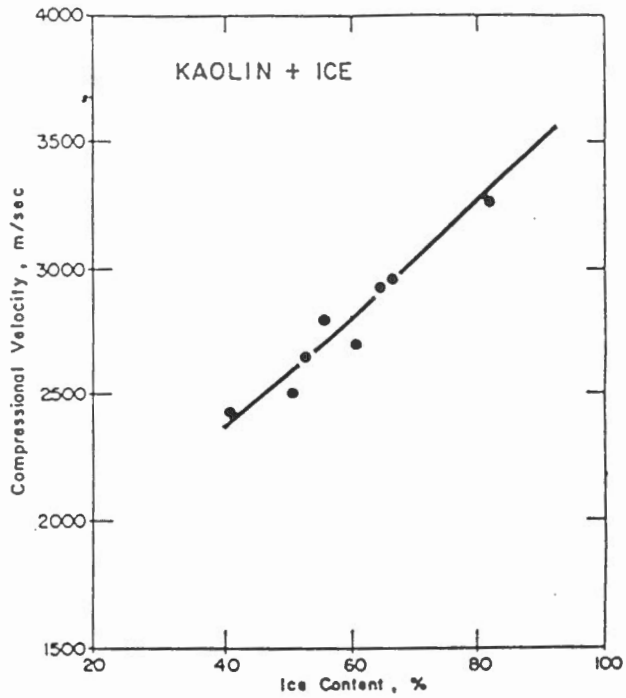
b. Velocity vs temperature (F.F. Aptikaev 1964).

Figure 1. Dependence of electrical resistivity and compression wave velocity on temperature and lithology.



a. Conductivity vs ice content (Hoekstra 1975).

Figure 2. Variation in resistivity and seismic velocity as ice content changes.



b. Velocity vs ice content (Frolov and Zykov 1971).

Figure 2 (cont'd). Variation in resistivity and seismic velocity as ice content changes.

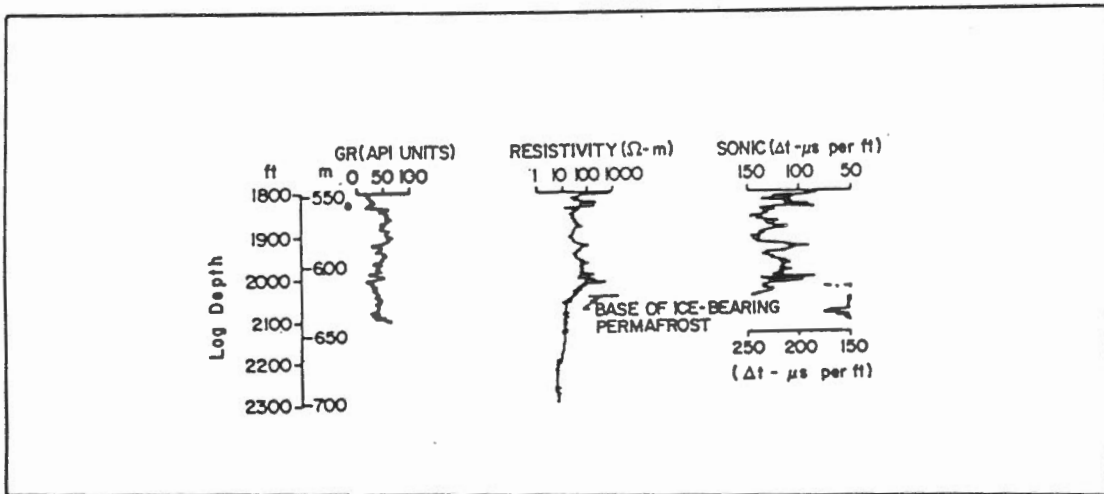


Figure 3. Resistivity and sonic logs, Prudhoe Bay (Osterkamp and Payne 1981).

Figures 1 and 2 were mainly compiled from laboratory testing of samples. Figure 3 illustrates in-situ measurements of electrical and acoustic properties performed in a well in the Prudhoe Bay area of Alaska (Osterkamp and Payne 1981). It is apparent that the substantial features of the resistivity log correlate to similar features on the sonic log. It can be concluded that:

- 1) Electrical methods may be used to delineate areas of permafrost, since the frozen state of the material alters its resistivity.
- 2) Information concerning the distribution of permafrost obtained from electrical methods may be used for the purpose of static correction to reflection seismic data, since both the electrical and elastic properties appear to be affected in similar manners by the presence of permafrost.

CASE HISTORIES

Three case histories are drawn from onshore and offshore regions in the western Canadian Arctic. One example shows the results of a TEM survey from the Alaskan North Slope.

All of the surveys described were performed using the Geonics EM-37 transient system. A nongrounded square loop was used as a transmitter. Figure 4 shows the survey arrangement. The survey in Alaska was carried out using a transmitter loop of 500 m by 500 m. The Canadian surveys were conducted with two transmitter loop sizes (400 m by 400 m and 100 m by 100 m) centered at a measurement station. Additionally, TEM data in the Canadian Arc-

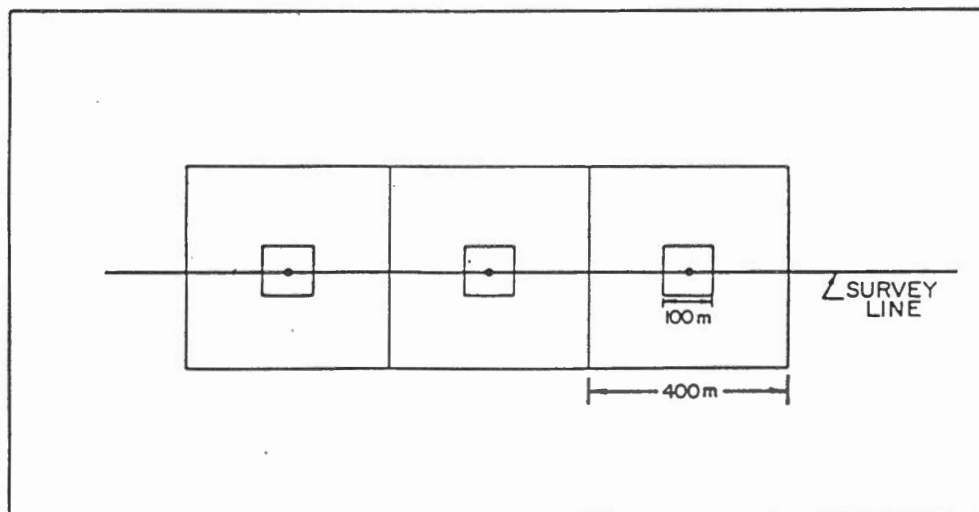


Figure 4. Survey array.

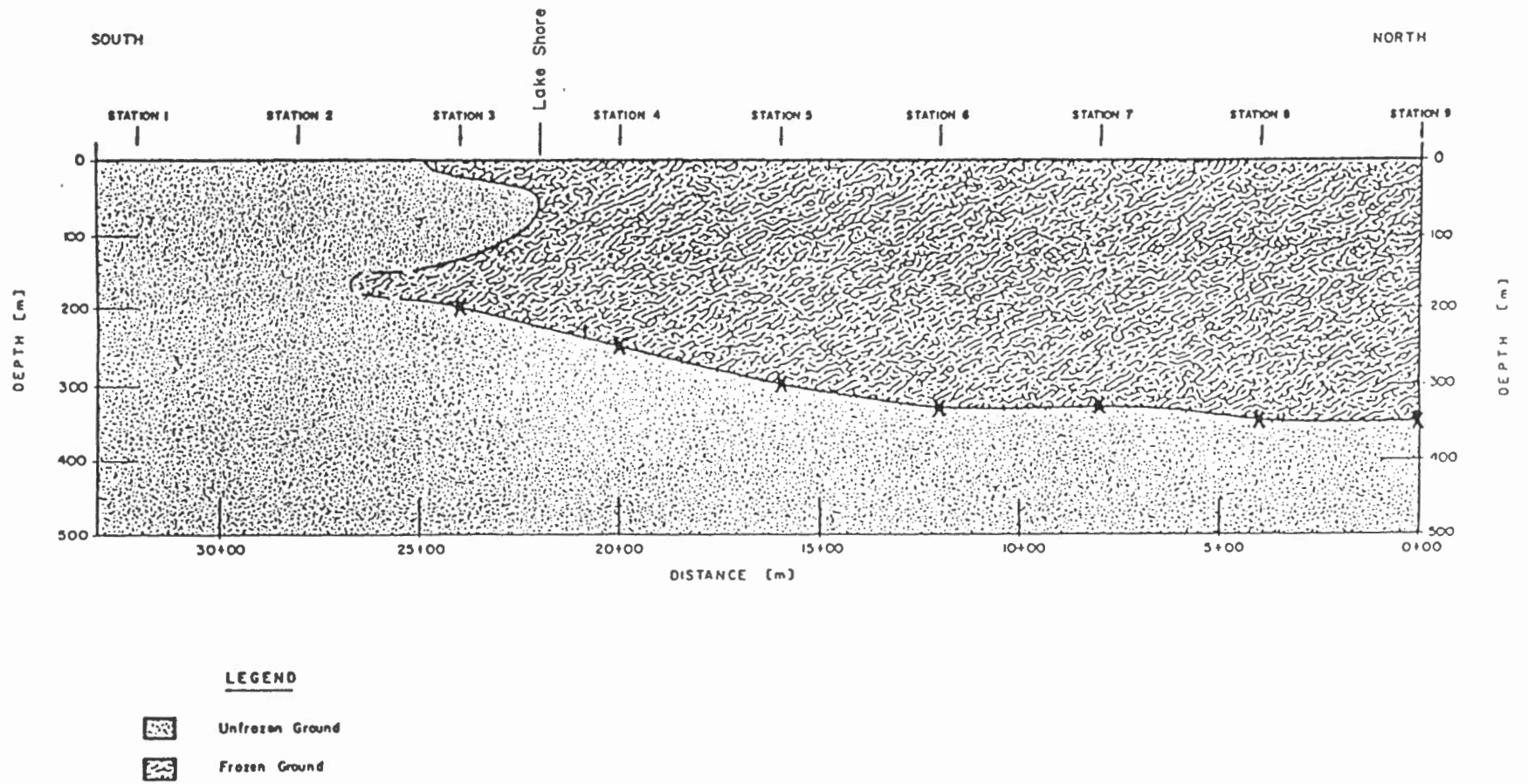
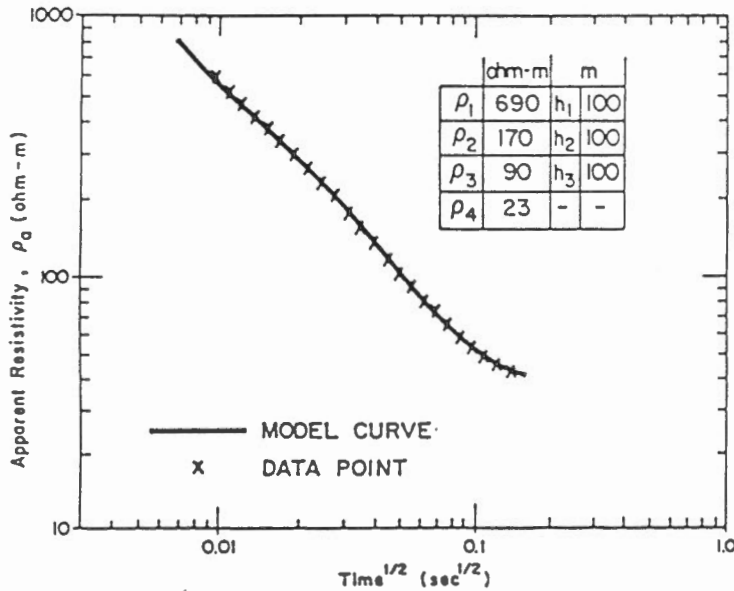


Figure 5. Interpreted section, case history 1.

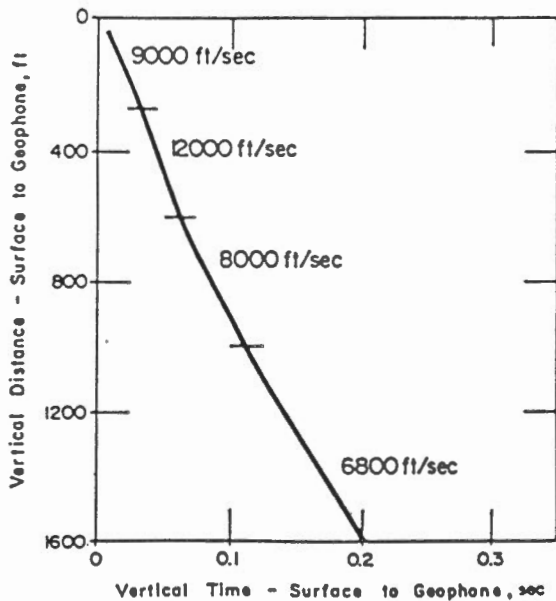
tic were supplemented by fixed frequency (EM) magnetic induction measurements, performed using the Geonics terrain conductivity meters, the EM31 and EM34-3.

Case History 1

Figure 5 shows the section interpreted from geophysical measurements along a survey line over part of a large lake and the uplands to the north of the lake. The lake shore is located between stations 3 and 4, as indicated on the profile.



a. Measured and modeled curves.



b. Near-surface velocity data.

Figure 6. Data for case history 1.

Measurements for stations located north of the lake indicate that the terrain is frozen to the ground surface. Although the objective of the survey was to map only the top and bottom of permafrost, an attempt was made to differentiate layering within the frozen materials. Figure 6a presents an example of the quantitative interpretation. The figure shows the measured apparent resistivities superimposed on the best fit model curve. Three layers with different resistivity are apparent within the permafrost at this site. The resistivity layering is expected to be due to variations in lithology, ice content, temperature, etc. It could also be expected that sonic velocity will vary similarly within the permafrost.

Figure 6b shows the crystal cable velocity log from a nearby well. Compared to the interpretation of the TEM data, it shows that a resistivity boundary is also a velocity boundary. The layers of different resistivity are characterized by different values of velocity.

The permafrost structure near the lake shore has been determined using a synthesis of both EM and TEM data. This was required to reliably map changes in the section occurring both in the shallow subsurface and at greater depth.

No frozen ground is expected beneath the lake. However, calculations do show that, if a frozen layer with a thickness of about 20 m occurred at depths of about 150 m, its presence would not be detectable with the TEM configuration used.

Case History 2

Figure 7 shows the section interpreted from TEM data along a survey line in the high Arctic. The portion of the survey line on shore is frozen to the ground surface. The interpretation of the onshore TEM data indicates that permafrost is not electrically homogeneous throughout its thickness. Figure 8a shows the interpretation of the apparent resistivity curve for station 7. Four distinct layers are recognizable within the permafrost. The variation in the thickness and resistivity of these layers suggests that a gradual change of resistivity with depth may take place. The electric log from a nearby well (Fig. 8b) illustrates the gradual change of resistivity with depth.

For survey stations located offshore the TEM data indicate that the section consists of a conductive zone overlying resistive materials. The resistivity of the conductive materials is about 0.5 ohm-m. The conductor is essentially composed of sea water.

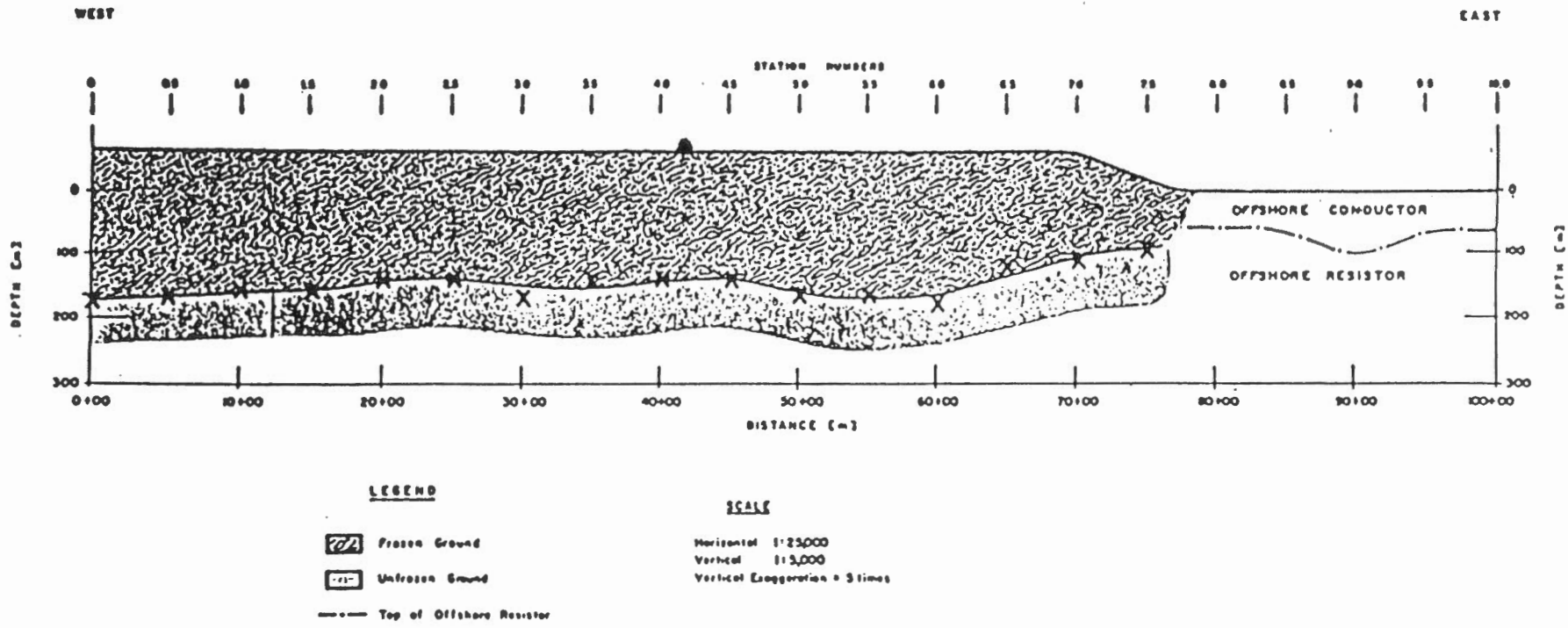
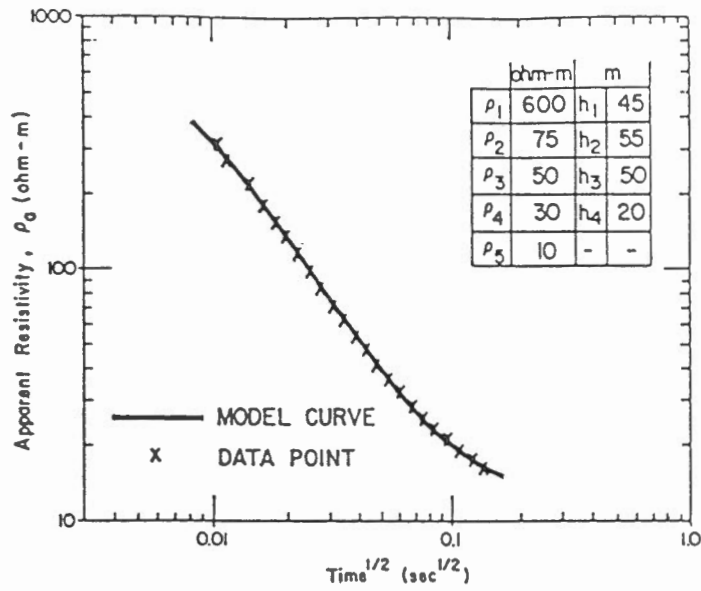
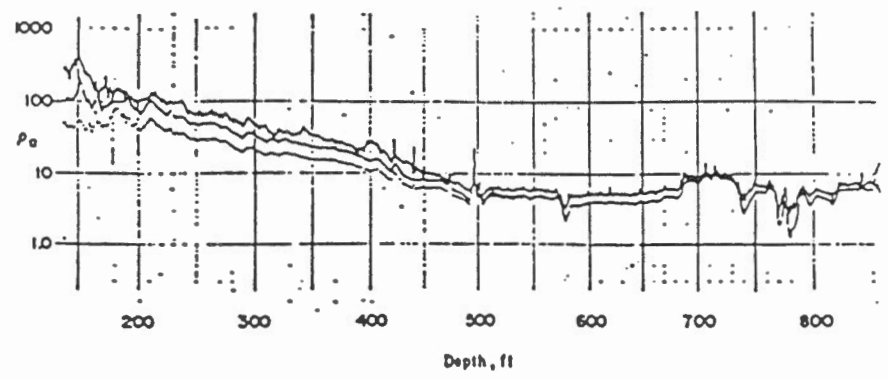


Figure 7. Interpreted section, case history 2.



a. Measured and modeled curves.



b. Resistivity log.

Figure 8. Data for case history 2.

The interpretation of the TEM data for offshore stations at this site indicates that water depth varies between 70 and 100 m. Since moderately resistive material (about 6 ohm-m) underlies the sea water, a resistivity contrast of up to 15 occurs at this interface. The occurrence of permafrost beneath the moderately resistive materials cannot be determined from data obtained using the present operation mode. The limits of detectability of permafrost beneath sea water depend mainly upon the resistivity and thickness of both the sea water and underlying unfrozen sediments.

Case History 3 (Ehrenbard et al. 1983)

Figure 9 shows a section interpreted from TEM data at a site on the North Slope of Alaska. Unlike the previous case history, it is possible to map offshore permafrost in this region. The data do not reveal as large a resistivity contrast with underlying unfrozen sediments so that the presence of permafrost and its thickness can be determined. The factors which allow the delineation of permafrost in this case are the shallower water (less than 10 m), the greater resistivity of sea water, the lower resistivity of unfrozen sediments, and the presence of a substantial thickness of permafrost.

Case History 4

Figure 10 shows a section interpreted from TEM and EM data along a survey line located in the Mackenzie Delta. In general, the section exhibits a four-layered structure: surface frozen sediments, intermediate unfrozen sediments, the main body of permafrost, and underlying unfrozen materials. At various locations along the survey line the four-layered structure degrades into a three-layered structure in which the upper frozen zone is absent, or a two-layered structure in which the intermediate unfrozen sediments are absent. Figure 11a shows the results of quantitative interpretation of sounding.

Figure 11b shows a crystal cable velocity log for a drill hole located close to station 1. It can be seen that electrical boundaries of permafrost correlate to the seismic boundaries. Figure 11c gives another example of a crystal cable velocity log to a greater depth.

This example illustrates the most complex distribution of permafrost encountered to date with TEM soundings. The role of data acquisition over such complicated sections is extremely important. Measurements taken with only one loop size, large enough to sense the bottom of permafrost, could not delineate the upper frozen zone. The use of two loop sizes, however, unambiguously indicates the presence or absence of this zone. Apart from the small-loop data, EM measurements have allowed the detection of a near-surface talik between stations 3 and 4 and the unfrozen "pockets" between stations 10 and 13.

Where the section is frozen to the ground surface and no intermediate unfrozen ground occurs, it is possible to differentiate between layers of different resistivity within the permafrost. Figure 11d shows that at least two distinct layers are present.

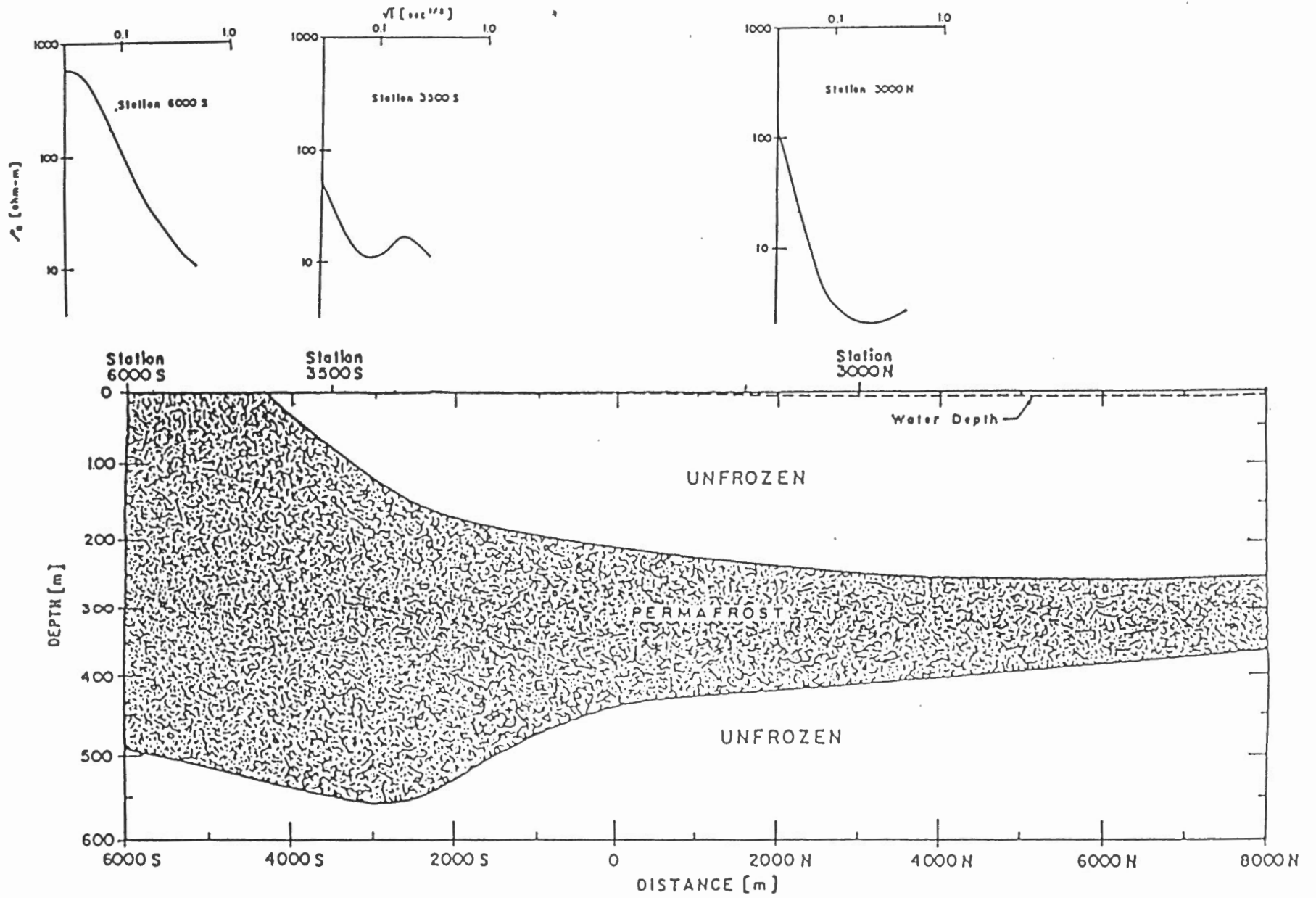


Figure 9. Interpreted section, case history 3.

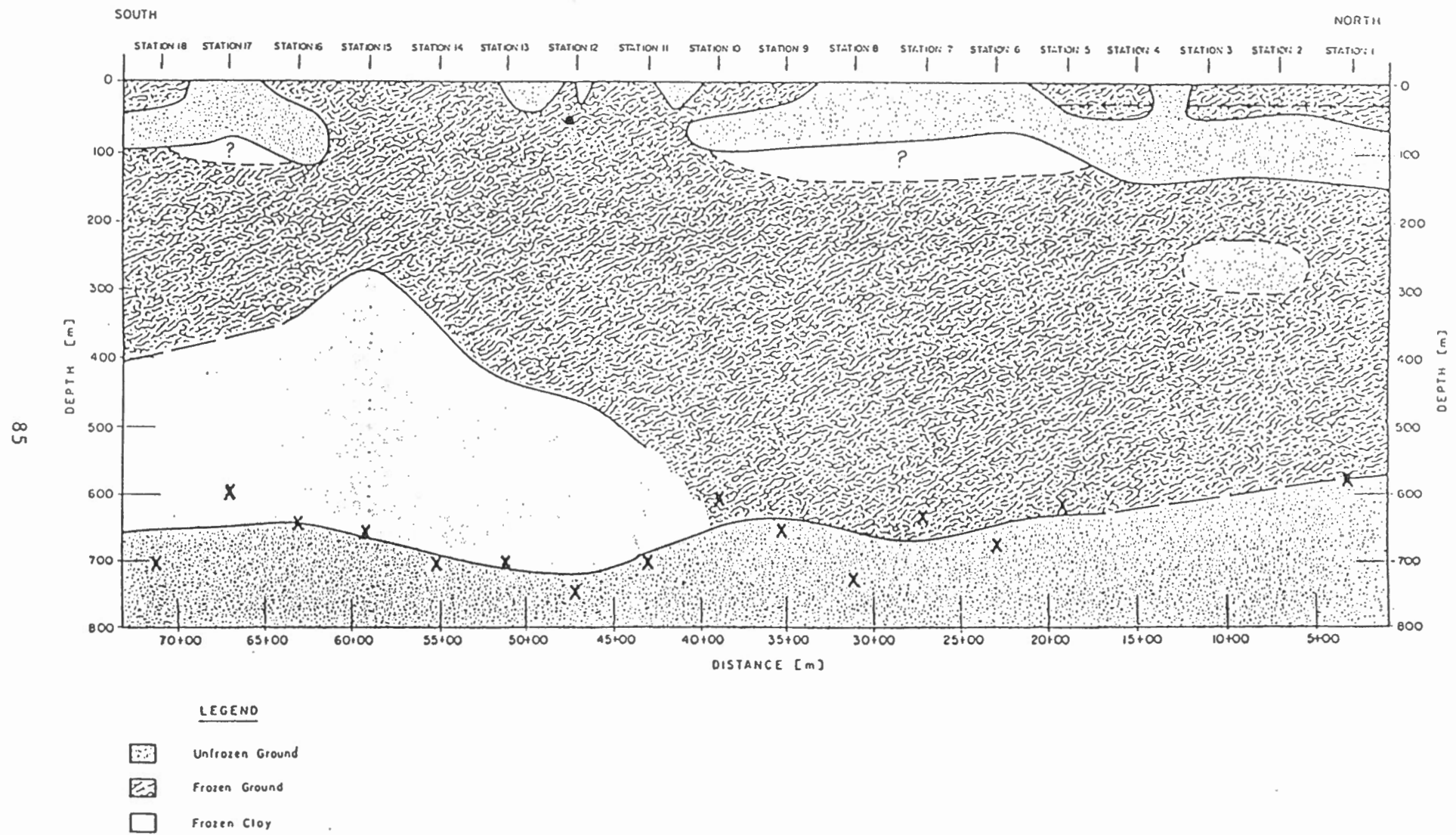
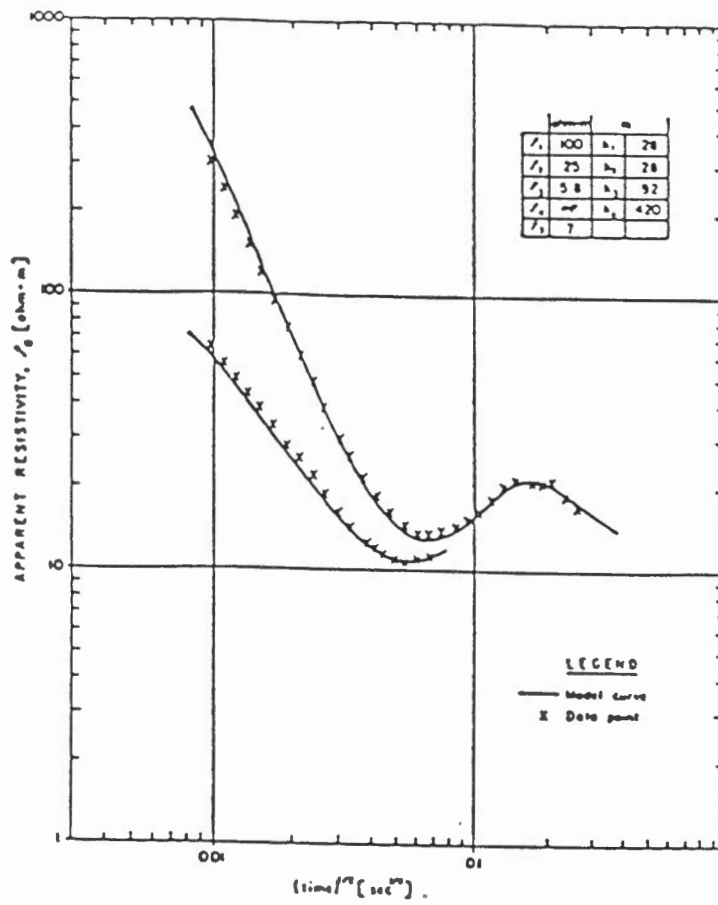
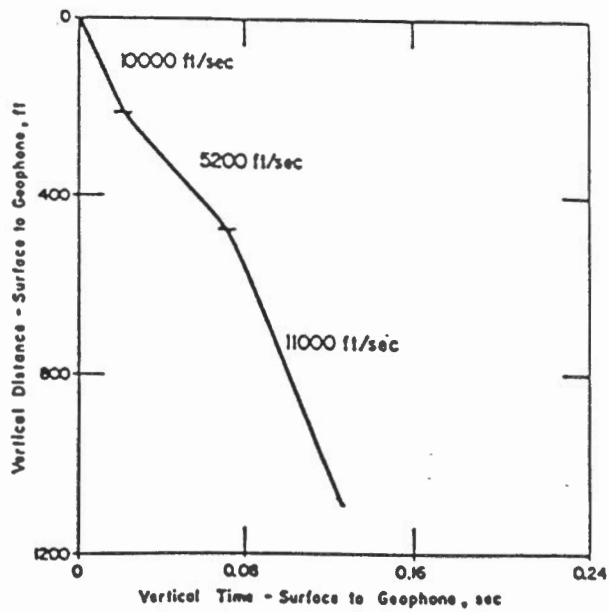


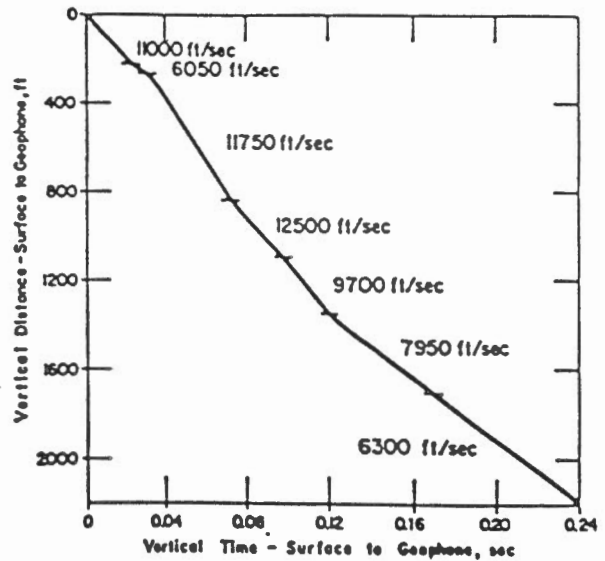
Figure 10. Interpreted section, case history 4.



a. Quantitative interpretation of sounding.

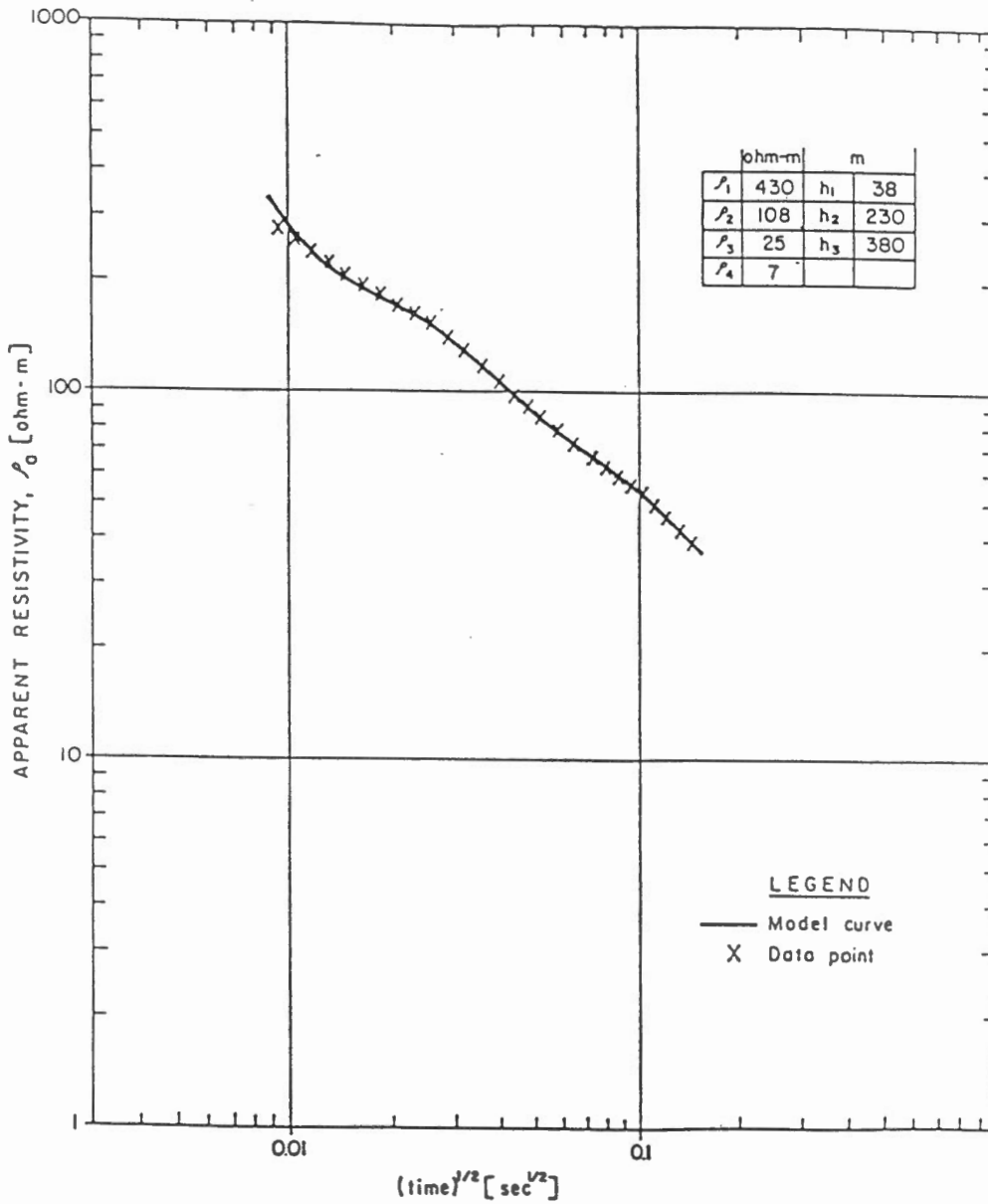


b. Near-surface velocity data.



c. Near-surface velocity data.

Figure 11. Data for case history 4.



d. Measured and modeled curves.

Figure 11 (cont'd). Data for case history 4.

The large "wedge" of material occurring south of station 10 is characterized by a resistivity of 25 ohm-m. This resistivity can represent, for example, frozen clay or unfrozen silt. Therefore, it is difficult to determine definitely the frozen state of material within this "wedge." Additional subsurface information is required to resolve this problem.

CONCLUSIONS

The case histories presented illustrate the flexibility of the TEM method to determine the presence and extent of permafrost under widely different geologic, geographic and geocryologic conditions. This flexibility is the result of two strong advantages of the TEM method over other electrical and electromagnetic techniques:

1) The method possesses strong vertical resolution, due to its high sensitivity to the geoelectric section.

2) The lateral resolution of the method is good, since the measurement array is small compared to the depth of investigation.

In many cases the method can not only map the top and bottom of permafrost, it can also detect the major variations of resistivity within the permafrost body. The comparison of TEM data with downhole sonic measurements has shown that changes in resistivity correlate to variations in sonic velocity.

In areas where there is a large variation in the upper portion of the geoelectric section, additional independent measurements with good resolving power at shallow depth should be gathered. It is our experience that TEM data at a smaller transmitter loop size and EM data at fixed frequencies can do much to complement the large-loop TEM data.

In marine environments the delineation of the extent of permafrost beneath sea water and unfrozen brine-saturated sediments can be a very complex problem. The important parameters are the thickness and resistivity of sea water conductive sediments, and the relative thickness of underlying permafrost. The limits of current resolution of the TEM method for this objective are known.

It has been shown that the frozen state of earth materials affects their electric and elastic properties in similar manners. This fact, along with the shown correlation between the resistivity and velocity layering, creates a good potential for using the electrical data at the stage of processing seis-

mic reflection data to make a reliable static correction for permafrost influence.

The information obtained by the TEM method can also be used for geotechnical and construction purposes, and in well planning.

ACKNOWLEDGMENTS

The authors express their deep gratitude to the scientific officers of the Gravity, Geothermics and Geodynamics Division, Earth Physics Branch, Department of Energy, Mines and Resources, Canada, for financial and moral support.

REFERENCES

- Aptikaev, F.F. (1964) Temperature field effect on the distribution of seismic velocities in the permafrost zone. Akad. Nauk SSSR Sibirskoe Otd-*ie*. Inst. Merzlotovedeniia. Teplovye Protssessy v Merzlykh Porod.
- Ehrenbard, R.L., P. Hoekstra and G. Rozenberg (1983) Transient electromagnetic soundings for permafrost mapping. Proceedings, Fourth International Conference on Permafrost. Washington, D.C.: National Academy Press, p. 272-277.
- Frolov, A.D. and Y.D. Zykov (1971) Peculiarities of the propagation of elastic waves in frozen rocks. Izv. Vysh. Ucheb. Zaved., Geol. Razvedka, no. 10, p. 89-97.
- Hatlelid, W.G. and J.R. MacDonald (1982) Permafrost determination by seismic velocity analyses. J. CSEG, 18(1): 14-22.
- Hoekstra, P., P.V. Sellmann and A. Delaney (1975) Ground and airborne resistivity surveys of permafrost near Fairbanks, Alaska. Geophysics, 40(4): 641-656.
- Kaufman, A.A. and G.V. Keller (1983) Frequency and Transient Soundings. Amsterdam: Elsevier.
- Osterkamp, T.E. and M.W. Payne (1981) Estimates of permafrost thickness from well logs in northern Alaska. Cold Regions Science and Technology, 5: 13-27.
- Rozenberg, G.S. and P. Hoekstra (1982) Transient electromagnetic soundings. Society of Exploration Geophysicists Technical Program, Abstracts, Dallas, Texas, p. 376-378.

- Sartorelli, A.N. and R.B. French (1982) Electromagnetic induction methods for mapping permafrost along northern pipeline corridors. Proceedings, Fourth Canadian Permafrost Conference, National Research Council, Canada, p. 283-295.
- Scott, W.J., P.V. Sellmann and J.A. Hunter (1978) Geophysics in the study of permafrost. Proceedings, Third International Conference on Permafrost, National Research Council, Canada, vol. 2, p. 93-115.
- Walker, J.M.D. and A.M. Stuart (1976) Determining extent of permafrost. Oil-week, May 31.